Форма № 24

Изучение осцилляций нейтрино в эксперименте JUNO
(Участие ОИЯИ)
Продление проекта на период 2021-2023 гг

Study of Neutrino Oscillations in the JUNO experiment
(JINR Participation)
Project extension for the period 2021-2023

Шифр темы: 02-2-1099-2010/2023 Study of Neutrino Oscillations (Project JUNO)

Направление: Физика частиц и релятивистская ядерная физика

Авторы от ОИЯИ:

N. Anfimov[1)], T. Antoshkina[1)], S. Biktemerova[1)], A. Bolshakova[1)], I. Butorov[1)], A. Chetverikov[1)], A. Chukanov[1)], S. Dmitrievsky[1)], D. Dolzhikov[1)], D. Fedoseev[1)], M. Gonchar[1)], Y. Gornushkin[1)], M. Gromov[1)], V. Gromov[1)], D. Korablev[1)], A. Krasnoperov[1)], N. Kutovskiy[2)], K. Kuznetsova[1)], Y. Malyshkin[1)], D. Naumov[1)], E. Naumova[1)], I. Nemchenok[1)], A. Olshevskiy[1)], A. Rybnikov[1)], A. Sadovsky[1)], D. Selivanov[1)], A. Selyunin[1)], V. Sharov[1)], A. Shaydurova[1)], V. Shutov[1)], O. Smirnov[1)], S. Sokolov[1)], A. Sotnikov[1)], M. Strizh[1)], V. Tchalyshev[1)], K. Treskov[1)], N. Tsegelnik[3)], V. Zavadskyi[1)], O. Zaykina[1)]

[1)] Dzhelepov Laboratory of Nuclear Problems (DLNP)
[2)] Laboratory of Information Technologies (LIT)
[3)] Bogolyubov Laboratory of Theoretical Physics (BLTP)

Руководитель проекта: Д.В.Наумов

Зам.руководителя: М.О.Гончар

Дата представления проекта в НОО _____

Дата НТС Лаборатории *23/04/2020 (ЛЯП)* Номер документа _____

Дата представления физического обоснования на семинаре Лаборатории: *13/04/2020(ЛЯП)*

Дата первого утверждения проекта _____ *(ЛЯП)*

Форма № 25

ЛИСТ СОГЛАСОВАНИЙ ПРОЕКТА

Изучение осцилляций нейтрино в эксперименте JUNO
(Участие ОИЯИ)
Продление проекта на период 2021-2023 гг

Study of Neutrino Oscillations in the JUNO experiments
(JINR Participation)
Project extension for the period 2021-2023

Шифр темы: 02-2-1099-2010/2023

Утвержден директором ОИЯИ	_____	_____
	подпись	дата
СОГЛАСОВАНО		
ВИЦЕ-ДИРЕКТОР ОИЯИ	_____	_____
ГЛАВНЫЙ УЧЕНЫЙ СЕКРЕТАРЬ	_____	_____
ГЛАВНЫЙ ИНЖЕНЕР	_____	_____
НАЧАЛЬНИК НОО	_____	_____
ДИРЕКТОР ЛАБОРАТОРИИ	_____	_____
ГЛАВНЫЙ ИНЖЕНЕР ЛАБОРАТОРИИ	_____	_____
РУКОВОДИТЕЛЬ ПРОЕКТА	_____	_____
ЗАМ. РУКОВОДИТЕЛЯ ПРОЕКТА	_____	_____
О Д О Б Р Е Н		
ПКК ПО НАПРАВЛЕНИЮ	_____	_____

Abstract

JUNO, a reactor antineutrino experiment under construction in China, aims to determine the neutrino mass hierarchy with median sensitivity corresponding to 3-4 standard deviations and measure lepton mixing parameters with record sub-percent precision level. There is also a rich physics program including searches for proton decay, search for SN neutrino, detection of geo-, atmospheric and solar neutrinos, as well as searches for physics beyond the Standard Model.

JINR plays a major role in this project. (i) JINR is responsible for design and production of high voltage units for JUNO large (20 inches) and small (3 inches) photomultipliers (PMTs). (ii) JINR contributes to the construction of the Top Tracker detector developing a mechanical support system, hardware and software for monitoring of Top Tracker scintillators, tracks reconstruction and data acquisition system (DAQ). (iii) Mass tests and commissioning of large PMTs with help of JINR's designed and produced brand new scanning stations. (iv) JINR contributes to the design and construction of JUNO's near detector — TAO. (v) JINR contributes to the software leading development of Global Neutrino Analysis (GNA) package, developing simulation, reconstruction and analyses modules. (vi) JINR is commissioning a data center dedicated to Monte Carlo production, data storage and processing for JUNO experiment. This data center is expected to be one of three European data centers managing JUNO data.

JINR made a major contribution to Daya Bay experiment, providing PPO dopant to its liquid scintillator, leading oscillation analysis and participating in event selection algorithms, reactor spectra measurement and searches for sterile neutrino. The JINR team plans to continue the oscillation analysis, search for sterile neutrino. The corresponding research work will be done in the form of activity since Daya Bay terminates data taking in 2020.

The qualification of JINR team can be confirmed by their co-authoring of peer-reviewed articles on the research subjects in the leading journals, talks on behalf of collaborations and review talks on major conferences, successful participation in various neutrino experiments (JUNO, Daya Bay, NOvA, BOREXINO, OPERA, NOMAD). Importance of the obtained results is manifested in The Breakthrough Prize in Fundamental Physics 2016 awarded to a number of JINR scientists. JINR fellows serve leading positions in the organizational structures of JUNO and Daya Bay.

JINR contributed to the JUNO project about 6M$. We request further 3.2 M$ for three years of the project extension 2021-2023 for a successful participation in JUNO and Daya Bay experiments. The details of this request are presented in relevant parts of the project below.

1 Introduction

This document reviews a short report and the proposal of JINR continuation of participation in the JUNO project and in the Daya Bay experiment.

JINR participation in the Daya Bay experiment was formalized in 2007 and continued till 2017 inclusively within theme 1099. From 2018 till 2020 major forces were concentrated on the JUNO project still continuing the Daya Bay experiment under the title "JUNO/Daya Bay project". Here we report on 2018-2020 activities of the JINR team.

Now, when the JUNO enters its construction phase, while Daya Bay terminates data taking in 2020, we propose a further consolidation on the JUNO project moving the

Daya Bay counterpart of our work to an activity. In 2021-2023 the project will be named “JUNO Project”.

JINR made important contributions to both Daya Bay and JUNO experiments in hardware, data analyses, papers preparation and presentations of the results at conferences, workshops and seminars.

In particular, JINR provided the PPO dopant for Daya Bay liquid scintillator and its oscillation analysis of 2016 was recognized as the Daya Bay’s official. Some members of the JINR team from Daya Bay were awarded The Breakthrough Prize in fundamental Physics for discovery of three neutrino oscillations and non-zero value of theta13 mixing angle.

JINR plays a major role in the JUNO project. (i) JINR is responsible for design and production of high voltage units for JUNO large (20 inches) and small (3 inches) photomultipliers (PMTs). (ii) JINR contributes to the construction of the Top Tracker detector developing a mechanical support system, hardware and software for monitoring of Top Tracker scintillators, tracks reconstruction and data acquisition system (DAQ). (iii) Mass tests and commissioning of large PMTs with help of JINR’s designed and produced brand new scanning stations. (iv) JINR contributes to the design and construction of JUNO’s near detector — TAO. (v) JINR contributes to the software leading development of Global Neutrino Analysis (GNA) package, developing simulation, reconstruction and analyses modules. (vi) JINR is commissioning a data center dedicated to Monte Carlo production, data storage and processing for JUNO experiment. This data center is expected to be one of three European data centers managing JUNO data.

The main motivation of the JUNO reactor antineutrino experiment is a determination of the neutrino mass hierarchy with median sensitivity corresponding to 3-4 standard deviations and measurement of lepton mixing parameters with record sub-percent precision level. There is also a rich physics program including searches for proton decay, search for SN neutrino, detection of geo-, atmospheric and solar neutrinos, as well as searches for physics beyond the Standard Model.

The document is organized as follows. The current status of the research is shortly reviewed in Sec.2. The proposed research project for 2021-2023, including the report for 2018-2020 term is summarized in Sec.3. The JINR team of the project is shown in Sec.4. SWOT analysis is summarized in Sec.5. List of publications prepared in the framework of the project during 2018-2020 is given in Sec.6. Finally, Sec.7 displays our financial requests for 2021-2023.

Notes on terminology and notations. In what follows when we sometimes use the term “precision” quantified with the standard deviation (σ), when the term “accuracy” would be more appropriate. Hopefully, this will not confuse the reader. The references are shown as footnotes.

2 Current status

Let us briefly review the current status of topics - subjects of the proposed research project. Exhaustive details on JUNO physics potential can be found in Ref.[1]

2.1 Neutrino mass ordering

The term “neutrino mass ordering” (MO) refers to establishing an appropriate ordering $m_3 > m_1$ or $m_1 > m_3$. There is no easy and cheap way to measure the ordering. The MO can be determined using the following observables.

(i) **Neutrino oscillation** probability is sensitive to the MO in both appearance and disappearance channels. The disappearance channel is insensitive to the CP-violation phase which is currently unknown. On the contrary, the appearance channel suffers from the degeneracy due to unknown CP-violating phase which biases the MO for neutrino energy of GeV range and the baseline of 700 km. At a larger baseline the degeneracy is relaxed due to an increasing matter effect.

JUNO[2] exploits the disappearance channel using reactor electron antineutrinos. Its data taking should begin in 2022 and in eight years JUNO should be able to determine the mass hierarchy at 3 standard deviations.

NOvA[3] and T2K[4] accelerator neutrino experiments are taking data and currently both favoring the normal mass ordering ($m_3 > m_1$) at about 1.9 standard deviations each. By 2025 NOvA expects a determination of MO varying between 0.5 and 5 standard deviations. The interval corresponds to the degeneracy due to an unknown CP-violating phase.

The DUNE[5], an accelerator neutrino experiment, should start data taking in 2026 with 50% of the beam power and 50% of the total detector mass. The final upgrade is expected in 2030. DUNE should be able to determine the MO at 5 standard deviations around 2028.

IceCube and its dense extension PINGU would be able to determine the MO using atmospheric neutrinos. PINGU expected to reach ~4σ median significance after 5 years of data taking. The starting date is unknown to us.

(ii) **Neutrinoless double beta decay** probability is sensitive to the MO. The effective neutrino mass $m_{\square\square}$ is expected to be of the order $(2,6)\times10^{-2}$ eV for the inverted mass ordering, and $(2,6)\times10^{-3}$ eV for the normal mass ordering. Current experiments do not provide competitive limits on the MO.

(iii) **Cosmology** provides limits on the sum of neutrino masses Σ_ν. One expects that $\Sigma_\nu \geq 0.06$ eV for the inverted MO and $\Sigma_\nu \geq 0.1$ eV for the normal MO. Current bounds on Σ_ν does not provide yet a competitive limit, while a further increase in the Σ_ν determination accuracy is proved to be significant. The key players here are CMB-S4[6] and CORE[7] experiments. Their data taking dates are not known to us.

(iv) **Beta decay experiments** are also sensitive to the MO since each neutrino

[1] https://arxiv.org/pdf/1507.05613.pdf
[2] https://iopscience.iop.org/article/10.1088/0954-3899/43/3/030401
[3] https://novaexperiment.fnal.gov
[4] https://t2k-experiment.org
[5] https://www.dunescience.org
[6] https://arxiv.org/pdf/1610.02743.pdf
[7] https://arxiv.org/abs/1706.04516

mass eigenstate produces a kink in the energy spectrum. The corresponding measurement is extremely challenging since a recorde energy resolution is required to resolve these kinks. The KATRIN experiment will not provide a competitive limit, while the Project-8[8] experiment, which will use the Cyclotron Radiation Emission Spectroscopy in order to determine the mass of the electron antineutrino, will be able to provide the competitive limit. We refrain from discussing the time scale.

Let us note, that while sensitivities of individual experiments might be below the 5σ discovery significance, the joint analysis of their data is known to improve the overall sensitivity to the MO at a rate more significant than the usual statistical averaging of the data. The main reason for that is a significant reduction of the degeneracy in parameters determination when data from different categories (i)-(iv) are combined.

This consideration was one of our motivations to develop JINR global analysis framework (GNA). Today, the global neutrino fits favor the normal ordering at 3.4σ[9]. Further details can be found in Ref.[10]

2.2 Accuracy of the lepton mixing parameters determination

Currently, the accuracy in the determination of the lepton mixing parameters can be summarized in Tab. 1, recalculated from Ref.[11]

parameter	1σ uncertainty/parameter, in %	JUNO improvement
Δm^2_{21}	2.6	< 0.6%
Δm^2_{32}	1.2 Sign undetermined	< 0.5% Determine sign
$\sin^2\theta_{12}$	6.3	< 0.7%
$\sin^2\theta_{23}$	5.5	
$\sin^2\theta_{13}$	3.8	
δ	16	

Table 1. Accuracy in today's determination of the neutrino Δm^2_{ij} and lepton mixing angles.

JUNO will improve the determination of Δm^2_{32}, Δm^2_{21}, θ_{12} measuring them with sub-percent precision.

Daya Bay, discovered in 2012 a non-zero value of θ_{13}, is still determining the field. Its final accuracy for θ_{13} determination is expected to 2.5%.

[8] https://arxiv.org/abs/1309.7093
[9] https://globalfit.astroparticles.es/2018/07/03/neutrino-mass-ordering/
[10] https://arxiv.org/pdf/1806.11051.pdf
[11] http://pdg.lbl.gov/2019/reviews/rpp2019-rev-neutrino-mixing.pdf

2.3 Proton decay

To explain the observed matter-antimatter asymmetry of the universe, baryon number violation is one of the requirements. There is no experimental evidence for baryon number violation.

The decay mode $p \rightarrow K^+\nu$ is favored by a number of SUSY GUTs which typically predict the lifetime of the proton to be less than a few $\times 10^{34}$ yrs. The search for this mode in a large water Cherenkov detector is hindered by the decay kinematics. The momentum of the K^+ in this two-body decay is 339 MeV/c (kinetic energy of 105 MeV), which is below the Cherenkov threshold in water. Today's best limit is $\tau(p \rightarrow K^+\nu) > 5.9\times10^{33}$ yrs at 90% C.L. reported by the Super-Kamiokande collaboration[12].

LS detector is able to observe this channel using a unique triple time coincidence signature of the decay. In general, LS efficiency is significantly higher than that of the Cherenkov detector. Due to the high efficiency in measuring this mode, JUNO's sensitivity will surpass Super-Kamiokande in only 3 years since its data taking.

2.4 SN neutrino

So far, neutrinos from a single SN1987A explosion were detected in 1987 by Kamikande II (12 events), IMB (8 events) and Baksan (5 events). 25 detected neutrinos in total.

SN observations with neutrinos potentially is a rich source of information about the collapsing mechanisms of stars, strong matter effects for neutrino oscillation, and independent determination of the MO.

New generation of large scale detectors able to detect hundreds or thousands of SN neutrinos will determine our understanding of SN processes.

JUNO 20ktons detector will be able to detect about 10 thousand SN neutrino in different channels, assuming SN at 10 kpc.

Also, JUNO will have 3σ sensitivity to diffuse supernova background (DSNB) in ten years of data taking.

2.5 Geo-, atmospheric and solar neutrinos

2.5.1 Geo-neutrino.

Geo-neutrino, electron antineutrino produced in decays oa long-lived radionuclides in the Earth interior, was discovered by KamLAND[13] and BOREXINO[14] experiments. Latest analyses reveal 169 and 53 events attributed to geoneutrinos in KamLAND and BOREXINO data, respectively.

The new emerging field of science, **neutrino geophysics**, requires much larger

[12] E. Kearns, talk presented at the ISOUP Symposium (2013).

[13] H. Watanabe, talk at Neutrino Geoscience 2019, Prague, "Geoneutrino measurement with KamLAND", https://indico.cern.ch/event/825708/contributions/3552210/attachments/1930535/3197332/HirokoWatanabe_NGS2019.pdf

[14] M. Agostini et al., Borexino collaboration, "Comprehensive geoneutrino analysis with Borexino", Phys. Rev. D 101, 012009 (2020) DOI: 10.1103/PhysRevD.101.012009

statistics, see a recent review[15] for more details. JUNO will collect about 400 geoneutrinos per year. In ten years JUNO will determine geoneutrino fluxes with 5% precision by collecting the largest sample of geoneutrino interactions.

2.5.2 Atmospheric neutrino.

Detection of atmospheric neutrinos adds sensitivity to the MO determination and octant of θ_{23}. PINGU and ORCA will exploit this opportunity fully, determining this direction of research. JUNO will make a modest contribution to the MO determination on the level of about 1σ via detection of atmospheric neutrinos. At the same time, JUNO will measure θ_{23} with 6% precision, providing an independent input for θ_{23} octant determination.

2.5.2 Solar neutrino.

Today the solar neutrino puzzle is understood as due to neutrino oscillation accounting for the matter effects. The remaining issues emerged recently are (i) the solar metallicity and (ii) lack of data in the energy interval corresponding to the transition from vacuum to matter dominated regimes.

JUNO will be able to collect every day 1000 events from ^{7}Be and 10 events from ^{8}B solar reactions. This will shed new light on the solar metallicity and the transition from vacuum to matter dominated regimes.

2.6 Physics beyond the Standard Model

There are lots of various searches for BSM physics. It is impractical to mention all of them here, given the short format of the document. We mention only the search for light sterile neutrino. The MiniBooNE experiment claimed to observe a hint for sterile neutrino in 2018[16]. Reactor antineutrino experiments observe about a 5% deficit with respect to modern models expectations. If interpreted as a hint for sterile neutrino, the fourth neutrino mass should be of eV range scale.

Recently, Neutrino-4 collaboration claimed[17] to observe sterile neutrino with mixing parameters $\sin^2\theta_{13}=0.35$ and $\Delta m^2_{32}=7.5$ eV^2.

Direct searches by Daya Bay, MINOS[18], DANSS[19] and other experiments did not find any evidence for the sterile neutrino existence, excluding part of the parameter's space. The large mixing angle claimed by Neutrino-4 is ruled out by Daya Bay.

JUNO both far and near detectors will be sensitive to sterile neutrino.

[15] O.Smirnov, "Experimental aspects of geoneutrino detection: Status and perspectives", Progress in Particle and Nuclear Physics 109 (2019) 103712. https://doi.org/10.1016/j.ppnp.2019.103712

[16] Aguilar-Arevalo, A.A.; Brown, B.C.; Bugel, L.; Cheng, G.; Conrad, J.M.; et al. (2018). "Observation of a significant excess of electron-like events in the MiniBooNE short-baseline neutrino experiment". *Physical Review Letters*. **121** (22): 221801. arXiv:1805.12028. doi:10.1103/PhysRevLett.121.221801. PMID 30547637

[17] https://arxiv.org/abs/1809.10561

[18] https://arxiv.org/abs/2002.00301

[19] https://arxiv.org/abs/1911.10140

3 The project

Main objectives of JUNO experiment are (i) determination of neutrino mass ordering; (ii) determination of Δm^2_{32}, Δm^2_{21}, θ_{12} with sub-percent precision; (iii) search for proton decay; (iv) search for SN neutrino; (v) detection of geo-, atmospheric and solar neutrinos; (vi) searches for physics beyond the Standard Model.

Main objectives of Daya Bay experiment are (i) the ultimate precision measurement of θ_{13}; (ii) most accurate measurement of reactor antineutrino spectra.

3.1 Experimental setup and research methods

The JUNO central detector (CD), displayed in Fig. 1, is a spherical acrylic tank with 35m diameter filled with 20 ktons of liquid scintillator (LS). The scintillation light is detected by about 18k 20'' PMTs (LPMT) and about 26k 3'' PMTs (sPMT) providing about 78% surface coverage.

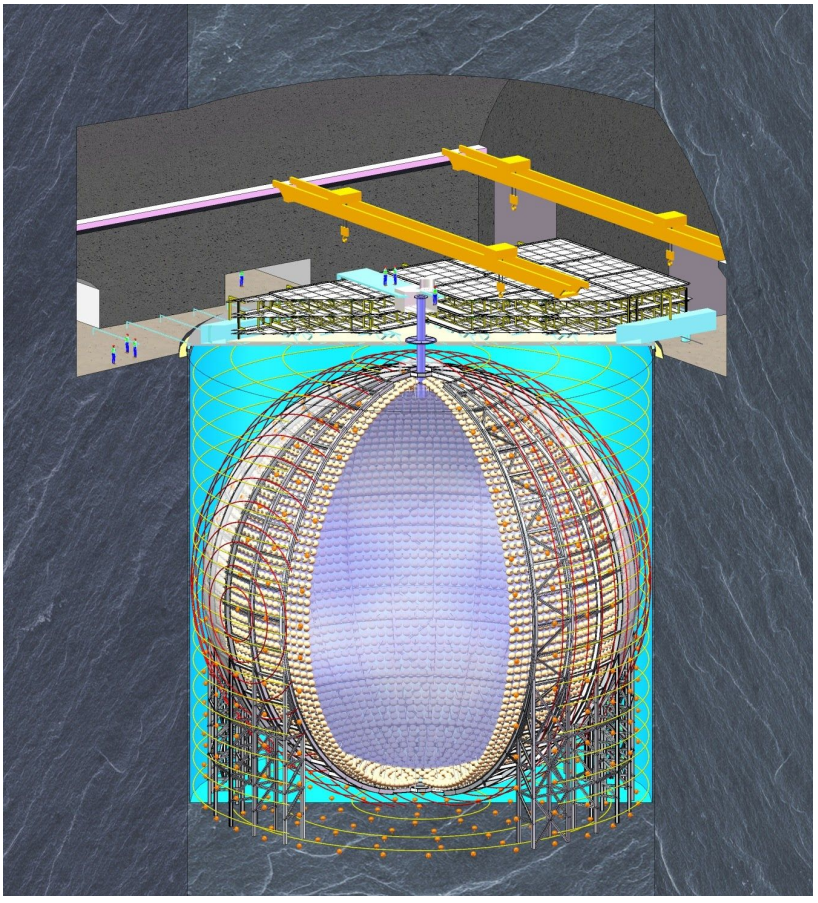

Figure 1. JUNO Central detector and its Top Tracker. The CD acrylic sphere diameter is about 35m. The CD is surrounded by a set of Helmholtz coils to compensate for the Earth Magnetic Field (EMF).

The CD is placed at 52 km from Yangjian and Taishan NPP with a total power of 26.6 GW.

In eight years of the data taking JUNO will collect about 100k of inverse beta decay (IBD) events determining the antineutrino energy with precision better than 3% at 1 MeV of the energy visible in the LS. The precise measurement of the IBD energy spectrum allows the determination of the neutrino mass ordering as can be seen in Fig. 2. and Fig. 3.

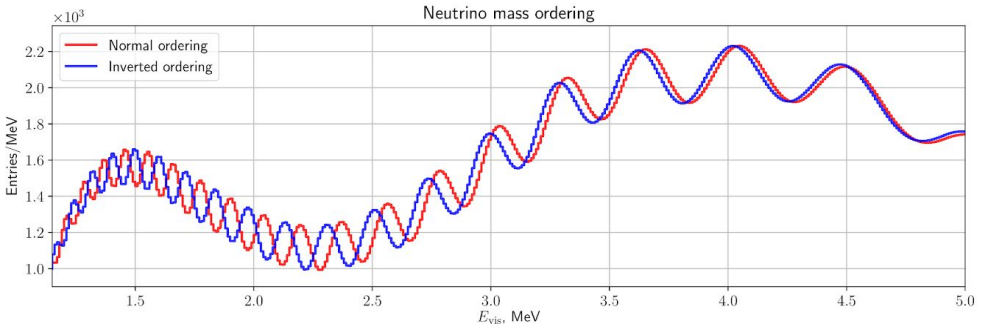

Figure 2. Expected energy spectrum in JUNO CD in eight years of data taking in two models of the mass ordering. The plot corresponds to the true energy.

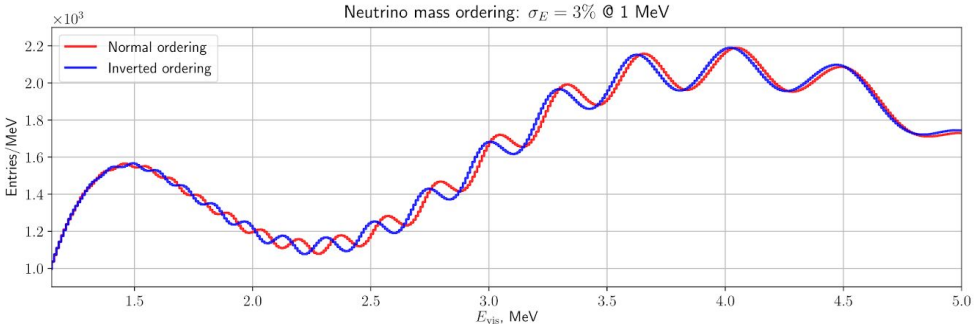

Figure 3. Expected energy spectrum in JUNO CD in eight years of data taking in two models of the mass ordering. The plot corresponds to the reconstructed energy, σ(E)=3% @ 1MeV.

The main challenge of this method is the energy resolution which should not be worse than 3% at 1 MeV of visible energy.

Another issue which was raised in recent years is a possible fine structure in the reactor energy spectrum. If present it might potential bias the wrong mass ordering and/or deteriorate the sensitivity of the experiment.

Therefore, the JUNO Collaboration decided to build a near detector JUNO-TAO which could measure the energy spectrum of reactor antineutrino with precision even better than in the JUNO CD.

The Taishan Antineutrino Observatory (TAO, also known as JUNO-TAO) is a satellite experiment of the Jiangmen Underground Neutrino observatory (JUNO). TAO consists of a ton-level liquid scintillator (LS) detector at ~30 meters from the core of the Taishan power plant in Guangdong, China. About 4500 photoelectrons per MeV could be observed by instrumenting full coverage (~ 10 m^2) of Silicon photomultiplier (SiPM) of >50% detection efficiency, resulting in an unprecedented energy resolution approaching the limit of LS detectors.

The detector operates at -50 °C to lower the dark noise of SiPM to acceptable level. The TAO experiment is expected to be online in 2022. The main purposes of the TAO experiment are

1. to provide a reference spectrum for JUNO in determining the neutrino mass ordering[20], and eliminate the possible model dependence due to fine structures in the

[20] Neutrino Physics with JUNO. By JUNO Collaboration (Fengpeng An et al.). [arXiv:1507.05613 [physics.ins-det]]. 10.1088/0954-3899/43/3/030401. J.Phys. G43 (2016) no.3, 030401.

reactor neutrino spectrum;

2. to provide a benchmark measurement to test nuclear databases, by comparing the measurement with the predictions of summation method;

3. to provide increased reliability in measured isotopic antineutrino yields due to a larger sampled range of fission fractions;

4. to provide an opportunity to improve nuclear physics knowledge of neutron-rich isotopes[21];

5. to search for light sterile neutrinos with a mass scale at 1 eV;

6. to provide increased reliability and verification of the technology for reactor monitoring and safeguard.

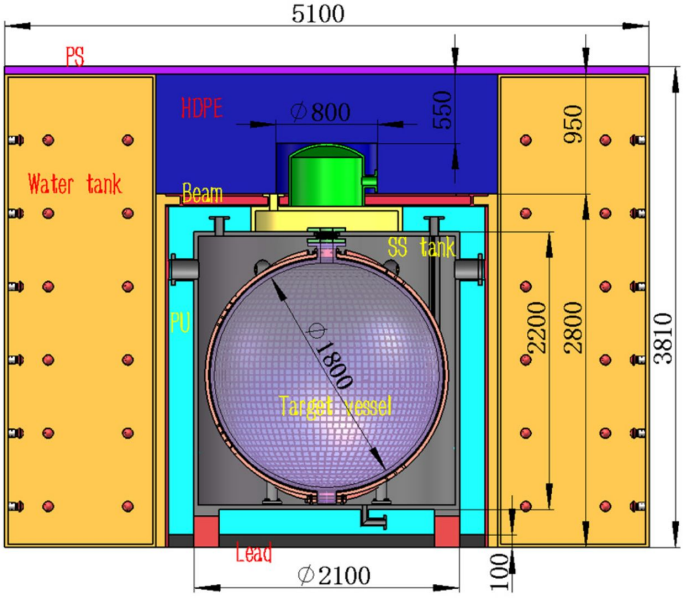

Figure 4. Schematic view of the TAO detector.

The schematic drawing of the TAO detector is shown in Fig. 4. The detector uses 2.8 ton gadolinium-doped LS (GdLS) contained in a spherical acrylic vessel of 1.8 m in inner diameter. To contain the gamma energy from the positron annihilation of the inverse beta decay (IBD) reaction, a 25-cm selection cut will be applied for positron vertex from the acrylic vessel, resulting in 1 ton fiducial volume.

The IBD event rate in the fiducial volume will be 2000 (4000) events per day with (without) detection efficiency taken into account. The scintillation light is viewed by 10 m^2 SiPM of photon detection efficiency higher than 50%. The detector has to operate at -50 degrees Celsius or lower to reduce the dark noise of SiPM to 100 Hz/mm. SiPM tiles are installed on the inner surface of a spherical copper shell of 1.882 m in inner diameter. The gap between the SiPM surface and the acrylic vessel is about 2 cm. The copper shell is installed in a cylindrical stainless steel tank of an outer diameter of 2.1 m and height of 2.2 m.

The stainless steel tank is filled with linear alkyl benzene (LAB), also the solvent of the GdLS, which serves as the buffer liquid to shield the radioactivity of the outer tank, stabilize the temperature, and couple optically the acrylic and SiPM surface. The stainless steel tank is insulated to operate at -50 °C as a whole. The detector is surrounded by a 1.2 m thick water tank on the side and a 1.2 m thick high density

[21] M. Fallot, B. Littlejohn, and P. Dimitriou. Antineutrino spectra and their applications, 2019.

polyethylene (HDPE) on the top to shield the ambient radioactivity and cosmogenic neutrons.

Cosmic muons will be detected by the water tank with PMTs instrumented and by plastic scintillators on the top. Although 3%/√E[(MeV)] energy resolution will be enough for TAO to serve as a reference detector of JUNO, as high as possible energy resolution is desired to study the fine structure of the reactor antineutrino spectrum and serve as a benchmark to test nuclear databases.

New findings might be achieved with a state-of-the-art detector. A light yield of about 4500 photoelectrons per MeV is expected for TAO by simulation, corresponding to an energy resolution of 1.5%/√E[(MeV)] in photoelectron statistics. However, when approaching the limit of the energy resolution of the LS detector, non-stochastic effects become prominent. At low energies, the contribution from the LS quenching effect is quite large, although it is not very well understood thus model dependent. At high energies, the smearing from neutron recoil of IBD becomes dominant.

Taking into account the projected dark noise, cross talk, and charge resolution of SiPM, the expected energy resolution of TAO is shown in Fig. 5. The usual 1/√E behavior is not valid here.

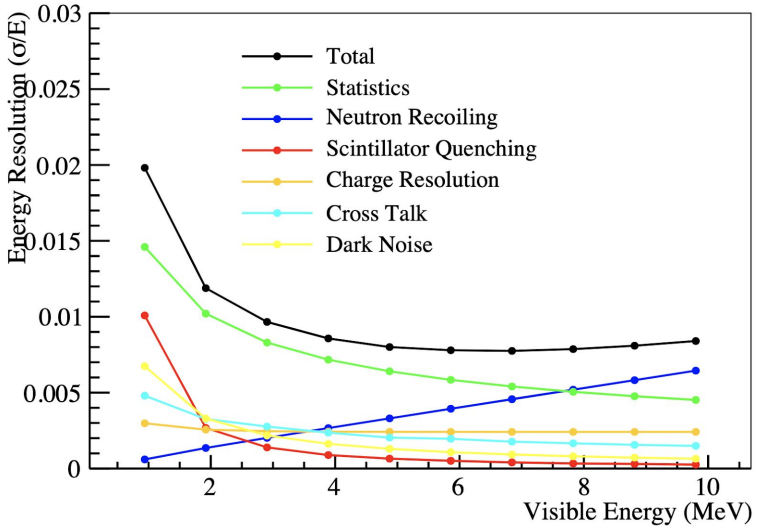

Figure 5. Expected energy resolution of TAO detector.

Taishan nuclear power plant is located in Chixi town of Taishan city in Guangdong province, 53 km from the JUNO experiment. It has two cores currently in operation. Another two cores might be built later. All cores are EPR reactors of 4.6 GW thermal power. At ~30 meter baseline, the event rate contribution in the TAO detector from the far core is about 1.5% of the total rate. The laboratory for the TAO detector is in a basement at 9.6 m underground outside of the concrete containment shell. Muon rate and cosmogenic neutron rate are measured to be 1/3 of that on the ground. Simulation shows that cosmogenic fast neutron background, accidental background, and cosmogenic ^{8}He/^{9}Li background can be well controlled to < 10% of signal with proper shielding and muon veto.

The detector R&D was started two years ago. A LS recipe has been developed and showed good transparency and light yield at -50 °C. SiPM has also been tested at the same temperature. A prototype is being tested at -50 °C.

3.2 JUNO at JINR

The JINR group in the JUNO experiment is from the very beginning of the project and is responsible for several of the key hardware and software developments.

In particular: the JINR group developed experimental procedures, designed and constructed test equipment and together with German and Chinese groups is responsible for the mass testing of 20'000 large 20" PMT to be installed in CD and Water Cherenkov Veto of the JUNO detector.

The large intellectual and financial contribution is made in the HV system of the JUNO experiment electronics. The brand new HV Units were designed, tested and are being produced now. The design allows for a number of intellectual features, self monitored operation and is using schematic, components, production and test processes compatible with the JUNO experiment request of extremely high reliability.

There is also a large and manyfold contribution to the precision part of the JUNO Veto system - Top Tracker detector. Starting from the supply to JUNO of the plastic scintillator planes produced in the past for the OPERA experiment, the JINR group has added to this system the design and construction of the mechanical support system and is responsible for the long term monitoring of the scintillator planes and software development for DAQ and electronics.

The JUNO Collaboration has proposed recently to construct also a near detector - TAO, which will serve for better understanding of the details of the reactor antineutrino fluxes. The group from JINR is contributing to the TAO detector design, carefully following special development of SiPM photosensors for TAO and setting up test procedures. It is expected that ~50% of the total amount of SiPM for TAO will be provided by JINR.

Preparing for the analysis stage of the project the computing resources at JINR are set up and a software development is going on. Investment to the computing infrastructure is planned to be performed jointly with other neutrino experiments. One of the major software projects developed at JINR is the Global Neutrino Analysis (GNA), which was already efficiently used in the Daya Bay experiment. Also several Monte Carlo and reconstruction algorithms are developed by the JINR people.

In the following the JINR activities are described in some more detail.

3.3 High Voltage Unit: Status and Plans

One of the main JINR contributions to the construction of the JUNO experiment is the design and production of the HV electronics for all of the JUNO PMT: ~18000 LPMT and ~27000 sPMT in the CD and ~2000 LPMT in the Cherenkov Veto.

During previous years of the project the JINR has completed the design, prototyping and extensive tests of the HV Units (HVU) to be used in the JUNO experiment.

The designed HVU is a programmable module, which provides the bias voltage to the voltage divider, specific to the type of PMT (HAMAMATSU, MCP or HZC) used in JUNO. The high voltage is generated by a custom module that converts a 24V DC voltage to a high DC voltage using a cascade of Cockroft-Walton multipliers. Such a system does not need any HV cables or connectors. The module is equipped with an embedded microcontroller. It monitors all operations and provides a RS485 half-duplex

interface to the electronics Global Control Unit. The total number of modules to be produced for JUNO is ~20000 for LPMT, 3500 for sPMT (1 HVU for 8 sPMT) plus some reserve.

The properties of the HVU are:

- range of HV: 1500V-3000V in steps of 0.5V.
- ripple: 10 mVptp
- HV long term stability: 0.05%
- temperature coefficient: 100 ppm/◦C
- maximum output current: 300 μA

Since HVU is a part of electronics located under water near PMT and has no chance for repair or exchange, special attention was paid to the reliability of the design, components and production processes. This includes prototyping, components selection, development of factory test protocols and temperature accelerated ageing tests. In addition, materials used in HVU were tested for radioactivity.

All of the tests were passed successfully and HVU was found to be compliant with JUNO requirements. The design of HVU has been approved by the Collaboration in a series of reviews, which examined full correspondence to the requested parameters, especially the reliability. Finally, the Production Readiness Review was passed and the production contract was signed with the electronics factory in Shenzhen. Now we are halfway in the production process. Namely, all of the production and test processes were setup and a pre-production batch (500 pieces) has been produced. This batch is undergoing final tests of the performance, stability and reliability in JUNO electronics, LPMT and sPMT groups.

It is planned to finish the full production (25000 pieces) by the end of 2020. After that the JINR group will follow electronics assembly, tests and installation. We will also continue to work on the firmware of HVU and general JUNO slow control software development. Resources requested are for possible contract amendment and additional test equipment. They correspond to ~10% of the resources previously requested for the production.

3.4 Top Tracker

The JUNO Top Tracker detector will be built of the modules previously used in the OPERA experiment as the Target Tracker detector. JINR took an active part in the construction of the TT detector for the OPERA experiment and the data analysis during the experiment. Now JINR participates in the creation of the Top Tracker detector of the Veto system of JUNO. The supply of a former OPERA detector was already accounted as a JINR in-kind contribution.

In addition, the JINR group:

- is responsible for the design, fabrication and construction of the mechanical support of the TT detector;
- is responsible for monitoring of the performance of the TT modules during the period of their storage;
- takes part in a development of the data acquisition system software;
- takes part in the offline software development for the analysis of the TT data.

Assembly, installation and commissioning of the Top Tracker detector will begin in 2021 and will take 5-6 months. The participation of 4-5 JINR specialists is required for

this period.

3.4.1 Mechanical Support Design and Construction

The TT detector will be placed on top of JUNO, above the pool. It has three layers, and each layer consists of 21 «walls» which are composed of 8 TT modules, 4 by 4 in X and Y direction. The walls have a weight of about 1 t and a size of 7 by 7 m^2, so one layer is of about 1000 m^2. The TT detector layers will be supported by a mechanical structure (see in Fig. 6, 7). Its design has been developed by JINR and validated with the prototypes made in Dubna. The procedure of the walls assembly as well as the necessary auxiliary tools has been also developed and validated at JINR. Everything was approved by a dedicated JUNO Review Committees. The support structure will be produced by the industrial company chosen by a bidding procedure in 2019. The fabrication of the whole mechanical structure (about 140 ton) is supposed to begin in 2021. The TT assembly should start in October 2021 and to be completed in March 2022 .

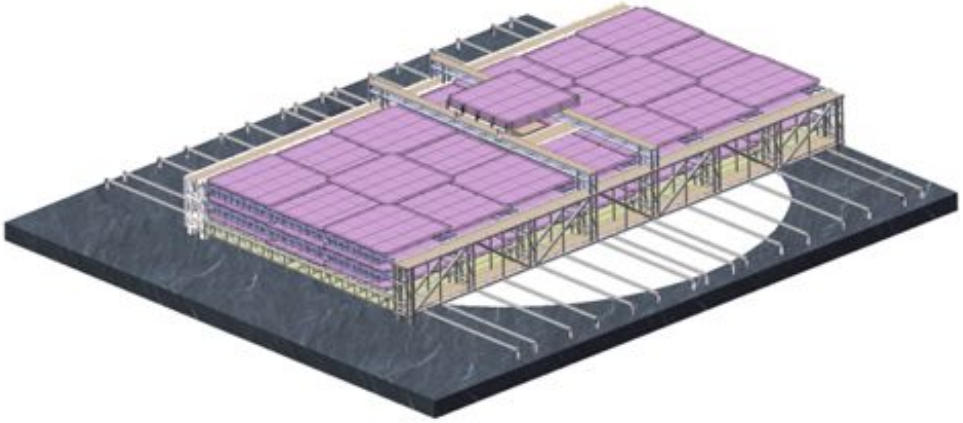

Figure 6. A general view of the TT detector.

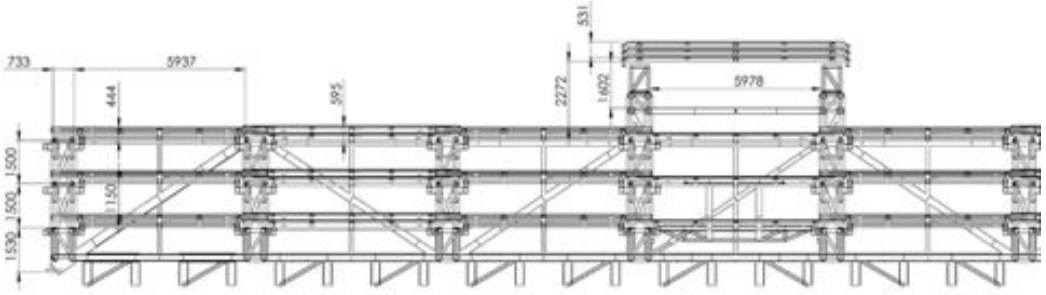

Figure 7. Drawings of the mechanical support.

3.4.2 Monitoring of the TT scintillators performance

The TT modules are made of plastic scintillator (PS) strips produced in 2003-2005. Plastic scintillator performance can degrade with time due to decrease of the light output and the PS transparency. In the OPERA experiment the performance of PS was monitored with help of muons registered by the detector. It was found that an amplitude of the signal, corresponding to the same energy deposit, slowly decreases by 1.7% per year. After dismantling the OPERA Target Tracker detector, the TT modules were placed in 7 containers and shipped to China where they are stored until the Top

Tracker assembly in 2021. The transportation from Italy to China by sea as well as storage for 4 years in South China can accelerate the scintillator aging, so its control is an important issue.

To control the performance of the TT modules directly in the storage containers, some of the modules are equipped with the DAQ electronics and can detect cosmic muons (Fig. 8). The detection of cosmic muons allows us to track a change in the detector response (Fig.9) with time. A special mobile DAQ and dedicated software have been developed at JINR.

The control of the TT modules response has been started already in Gran Sasso underground laboratory just after placing them in containers, thus providing a control point for further measurements. After arrival in China in summer of 2017, the containers were stored in two different places: until November 2018 - in a warehouse in Zhongshan and later at JUNO site (Kaiping). The data taking with cosmic muons goes on automatically under control via the internet.

Although the relative layout of the containers changed after each displacement, a comparison of the TT response to cosmic muons during 3 years shows no significant ageing effect so far (Fig. 10).

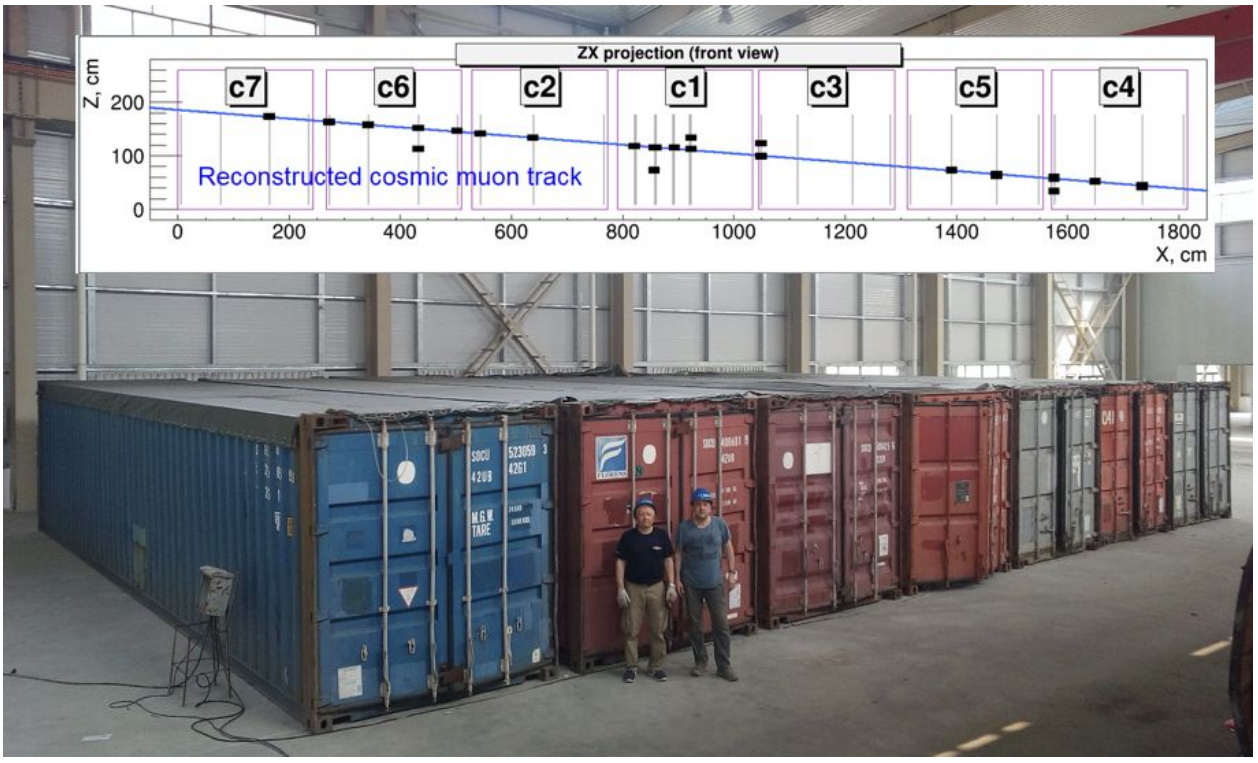

Figure 8. A general view of the containers with the TT modules at JUNO site. Example of reconstructed cosmic muon track passed through all 7 containers (top part).

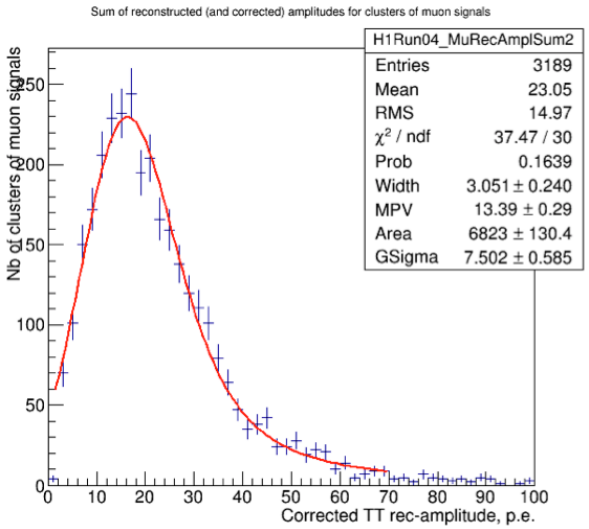

Figure 9. A distribution of the TT response on “horizontal” cosmic muons. A variation of the parameters (MPV and a mean value) with time is under control.

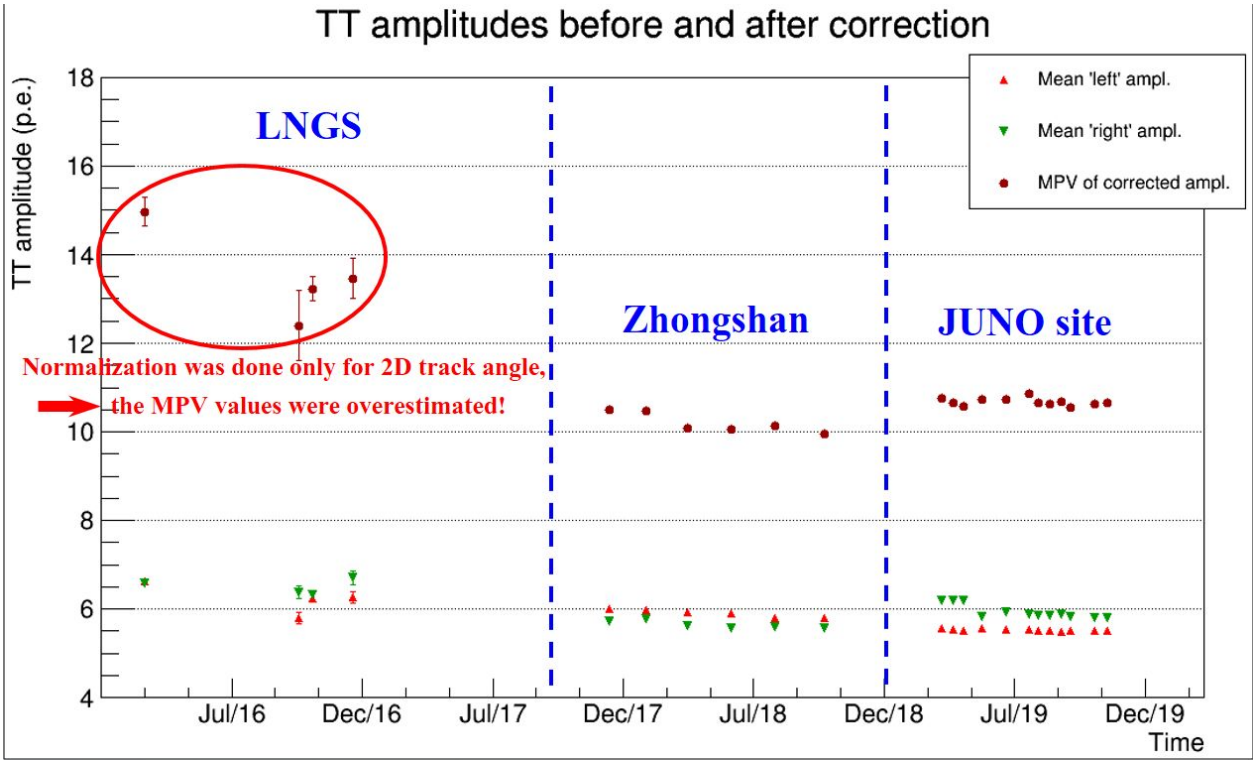

Figure 10. The corrected (normalized) TT amplitude of the strips response to muons (top). TT amplitude characteristics followed with time (bottom).

3.4.3 Data Acquisition System

To cope with a high signal rate (>50kHz per PMT) in the JUNO experiment, the TT detector will be equipped with new DAQ electronics : Front End (FE) cards, based on MAROC3 chip (designed by LAL, France) are being developed at IPHC in Strasbourg, new Readout Board (RB) are under design at CAEN (Italy) and additional units to suppress background at a hardware level: Concentrator Board (CB) and Trigger Board (TB) - both under development at IPHC (Fig. 11). JINR is responsible for the development of DAQ software which has to provide efficient data collection from the

detector. The pilot prototypes of FE, RB, CB are available at JINR and are being used for this task (Fig. 12). Also the cosmic ray detector prototype built at JINR will be in use when the final version of electronics will be available. The prototype will be upgraded to have 3 layers and to be similar to the real JUNO TT detector.

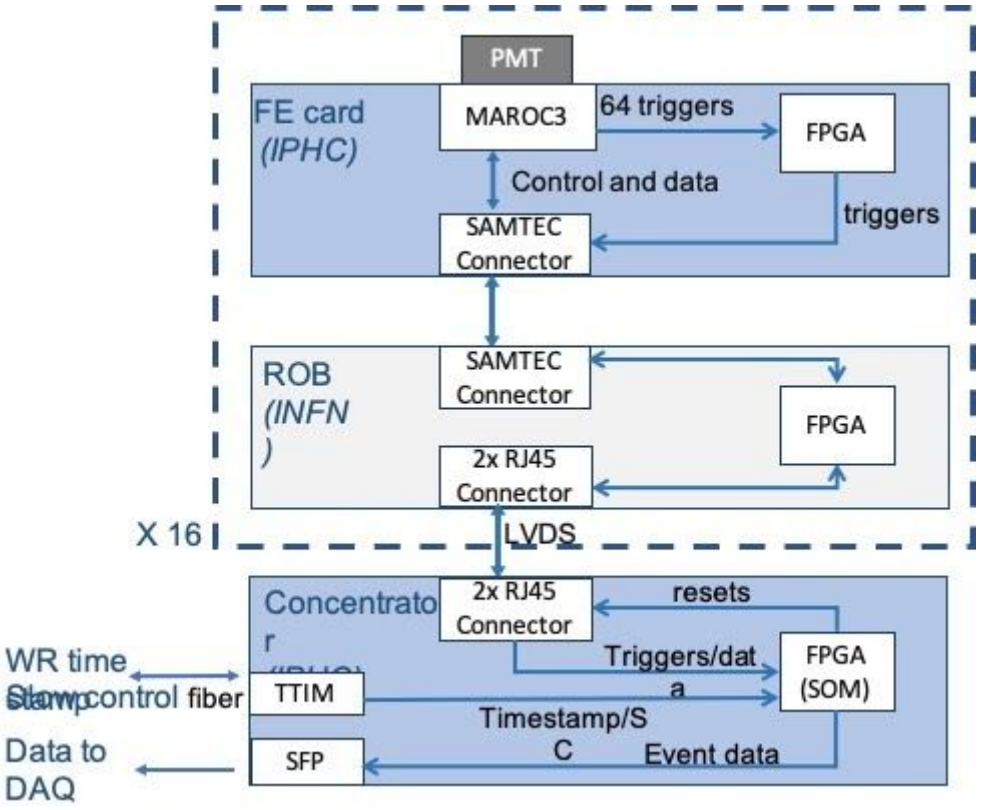

Figure 11. A scheme of the JUNO TT DAQ.

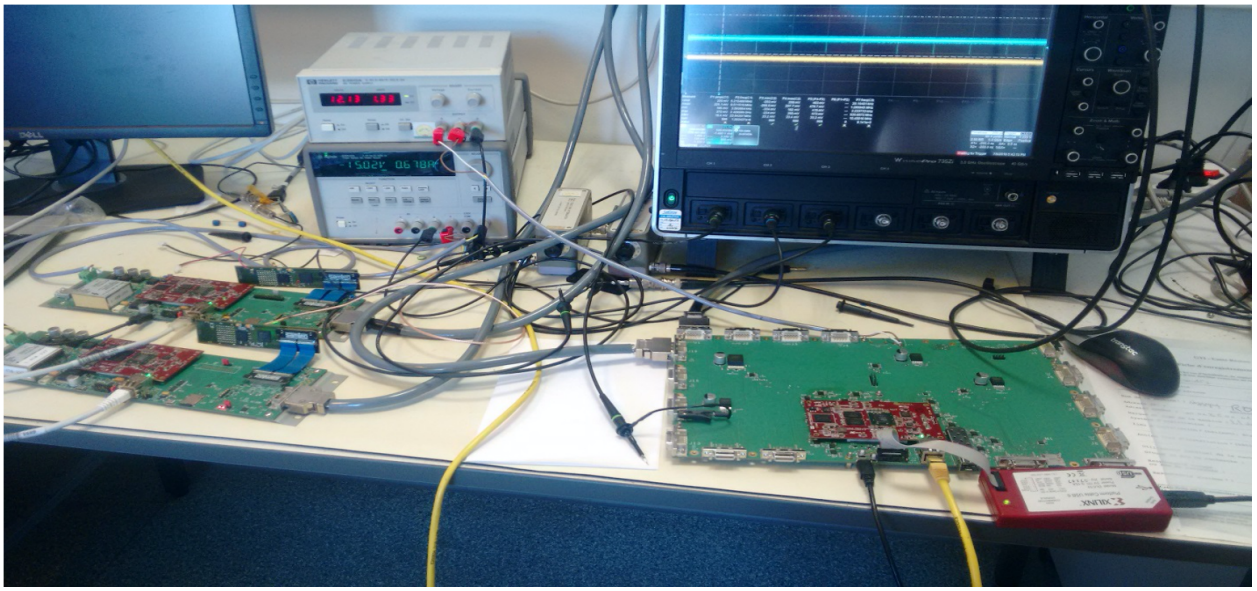

Figure 12. TT DAQ test bench.

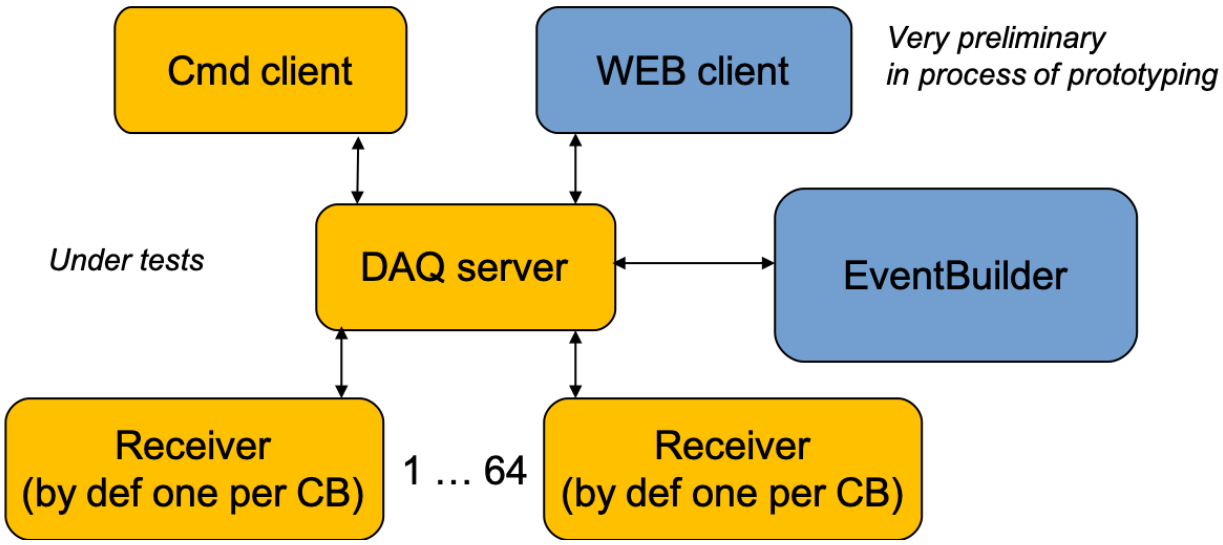

Figure 13. A Block-scheme of the TT DAQ software. The parts indicated in blue color are to be developed.

The DAQ and Slow Control (SC) software for JUNO TT is being developed in a paradigm of Distributed System Development (DSD). The applications responsible for a dedicated part of the process are being made standalone. The communication between applications is done with extensive use of ZeroMQ networking library - a powerful tool to handle the data and to provide the message exchange between different applications. It is chosen by JUNO Collaboration as a communication method for DAQ in the entire detector. The applications under development are: DAQ server, CB receiver, EventBuilder, DAQ control cmd client, DAQ control web client (Fig. 13).

The DAQ Server determines the status of the data collecting process: "Ready to start run" or "Run" or "Error received" etc. The state generated by the DAQ server is being propagated to all the Receivers. EventBuilder combines the segments of data collected by the CBs in one event. Command client and Web client both are the tools to control and configure DAQ server. Web client is supposed to be a main interface to the future JUNO TT shifters, while Command client is an auxiliary tool helpful while debugging. Some of those software elements (DAQ Server, CMD client, Receiver) already exist with several functionalities implemented. More functions will be added later. EventBuilder and Web client both are in a prototyping stage and will be developed in the next 12 months.

3.4.4 Software and data analysis.

The TT detector via providing a precise position of the muon tracks in the CD, can help to study the production of the cosmogenic isotopes like ^{9}Li/^{8}He in the interactions of the cosmic muons with the scintillator of CD. The layout of the TT detector (there are only 3 layers) and the presence of the random signals from the radioactivity, however, make this task not easy.

The algorithm for the muon track reconstruction in the TT is under development at JINR. Currently, the Monte Carlo simulation of the detector (partly at JINR, partly at IHEP computing batch system) is used. After equipment of the JINR TT prototype with a 3d layer and especially with a set of the real DAQ electronics, the algorithms can be validated with the data set very similar to the real data of the JUNO experiment. The combination of the TT data with the information from the Water Cherenkov detector to suppress the fake tracks due to an accidental noise in the TTcan increase the efficiency

of the muons reconstruction. The development of the related algorithms is under way as well. goal is also to combine information from the WP and CD about a rough position of the muon track.

3.5 Silicon photomultipliers for the TAO

The TAO detector is intended for precise measurement of the reactor antineutrino energy spectrum. With a yield of 4500 photoelectrons (p.e.) per MeV, the stochastic term of the energy resolution is 1.5%/√E[(MeV)]. In the energy region of the most interest, the expected energy resolution will be sub-percent. This dictates usage of more efficient photodetectors comparing the conventional photomultiplier tubes (PMTs).

A Silicon Photomultiplier (SiPM) is a good candidate, which is generally constructed as arrays of many very small Single-Photon Avalanche Diodes (SPADs). Each SPAD is integrated with its passive quenching resistor and all are connected in parallel. The SiPM works in Geiger mode and its output charge is the sum of all the elementary charges generated by each firing SPAD, which is proportional to the number of detected photons by the SiPM. The SiPM has relatively high photon detection efficiency, but also has huge thermal noise level at room temperature, compared to the PMTs. To decrease noise the TAO detector will operate at T = − 50 °C. This low operation temperature will lead to a drop of the thermal noise of about 3 orders of magnitude compared to the room conditions. Requirements on SiPM parameters.

Parameters	Specification	Comments
PDE	$\geq 50\%$	at ∼400nm, not include correlated noise
Dark noise rate	≤ 100 Hz/mm^2	at -50 degree
Probability of correlated noise	$\leq 10\%$	including optical cross talk and after pulse
Uniformity of V_{bd}	$\leq 10\%$	for the case w/o bias voltage tuning
Size of SiPM device	≥ 6 mm $\times$ 6 mm	for easy handling
SiPM coverage within tiles	$\geq 90\%$	not included in PDE

Table 2. SiPM parameters.

These assumptions were carefully checked by the MC simulation of the TAO detector see Fig. 14. It presents the required photon detection efficiency (PDE) of SiPMs to reach the reference energy resolution (1.65%, only statistics and ENF) under assumptions of different dark noise rate (y axis) and correlated noise (x axis). The parameters used in estimation of the reference energy resolution are also labelled in the figure. It is a trade-off between SiPMs' PDE and noises.

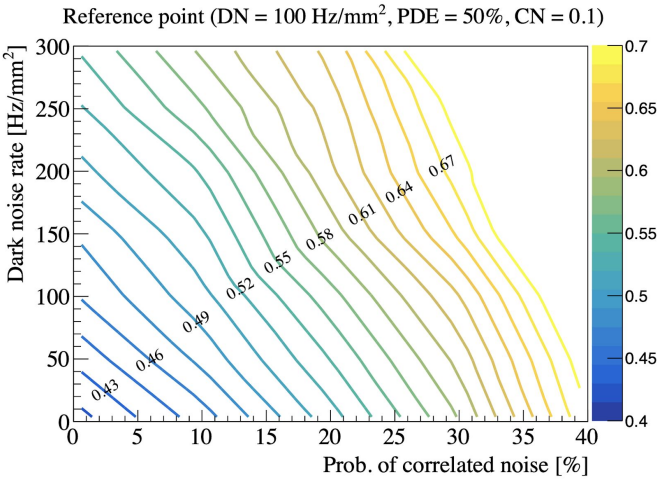

Figure 14. Figure of merit of the SiPM parameters.

3.5.1 SiPM tile

3.5.1.1 Requirements

A SiPM tile is used to support SiPM devices and provide connections for SiPMs to readout electronics. It consists of multiple SiPM devices and is a basic unit during detector installation. In SiPM tile design, the SiPM coverage within a single SiPM tile should be larger than 90% to ensure sufficient overall photon detection efficiency in the TAO detector. Meanwhile, the materials of the tiles should have good radio-purity since they are closed to the GdLS. The radioactivity requirements of SiPM tiles, together with readout electronics, should be less than 4.4 Bq/kg, 6.3 Bq/kg and 1 Bq/kg for Uranium, Thorium and Potassium, respectively. Moreover, the materials used by Tiles are required to be compatible with the LAB, in order to keep its good transparency. Different materials are under investigation as for SiPM tile assembly: Pyralux, Cuflon and other materials.

3.5.1.2 Tile design

There are two factors related to tiles that can contribute to the overall photon detection efficiency, and they can be optimized during the tile design. The first factor is the SiPM coverage within an individual tile. It depends on how to bond SiPMs on tiles. If Through Silicon Vias (TSVs) on the SiPMs are available, then a coverage close to 100% is expected. However, if the wire bonding has to be used to connect the front sides of SiPMs to the tile, then the coverage has to be reduced to leave space on tiles for bonding pads. After investigations on the existing technologies used by SiPM manufactures, we take the wire bonding option as a baseline in the tile design. A tile corresponding to the dimension of about 25 cm2 is the baseline design, consisting of 8 × 8 devices with sizes of 6×6 mm or 6×4 devices with sizes of 1 cm. The larger SiPM devices can also be used and we can gain a little bit higher coverage, however, SiPMs' yield on silicon wafers can be significantly reduced, which results in a high cost. With 6 × 6 mm^2 devices, if we leave 200 μm gaps for bonding pads and 100 μm gaps between devices, a coverage of about 95% can be achieved. More than 97% can be achieved with 1 cm. The second factor is the gaps between SiPM tiles. After some investigation of SiPM tile arrangement on the copper shell, we found the coverage of the SiPM tiles is about 94% by using tiles with rectangle shape and dimension of 5×5 cm. Regions at poles have smaller tile coverage, compared with regions at equator. However, if we use some irregular shape tiles, such as trapezoid, the coverage can be improved to about

96%, and, more important, the coverage uniformity on the copper shell becomes better. We take the irregular shape of the tiles as an alternative and more investigations are needed to make the final decision.The SiPM ganging can be implemented either in SiPM tiles or in front-end electronics boards. For both cases, the connections to SiPM devices will fan in to connectors on the back of tiles. However, for the former case, the connectors will have less pins, compared with that for the latter case.

3.5.1.3 Tile packaging

The SiPM devices are required to be enclosed for the purposes of protection and easy handling. The window material could be epoxy resin if LAB will be used as a buffer. If a liquid different from LAB will be used as a buffer, silicone resin can be used as window material. Some R&D efforts are needed to make the final selection. The normal FR4 PCB boards cannot be used to fabricate the tiles, due to its high radioactivity. Some low background materials that are suitable for tile fabrications are under investigations like Pyralux, Cuflon and other materials. A similar material will be used even for Front End board PCB.

The main JINR contribution to JUNO-TAO is to provide fundings for purchasing ½ of the total number of SiPM tiles. This number estimates around 1.5 M$.

3.5.2 SiPM power supply

One of the main JINR responsibilities in the TAO detector is to develop and provide a power supply for about 4500 SiPM arrays.

There are two possibilities to bias SiPM with reverse voltage. Schematically for some particular SiPM it is shown Fig. 15. All values of the component are used just for demonstration. The first approach is to use unipolar power and apply voltage from one side Fig. 15 (left) and the second one applies bipolar voltage from different sources from both sides Fig. 15 (right)

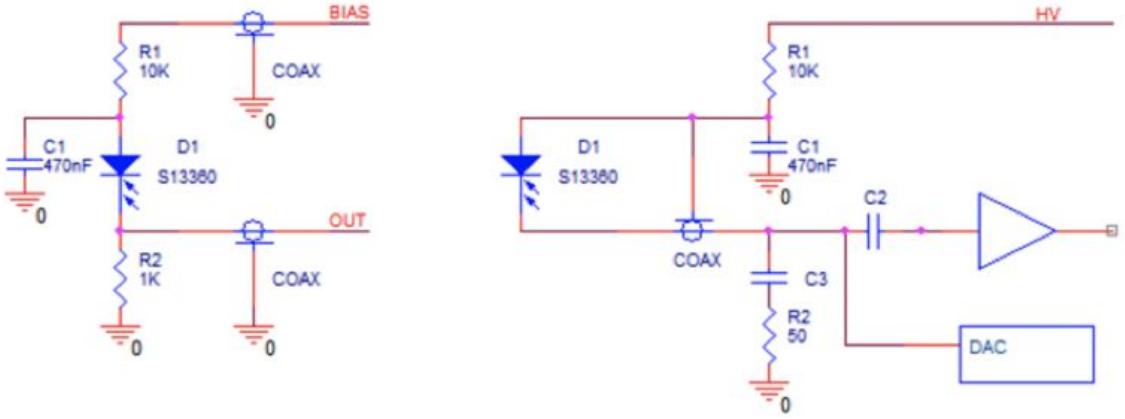

Figure 15. Schematics of a SiPM biasing. All values of the component are just for indication. Left - biasing from one side with unipolar voltage source. Right - biasing from two sides with two sources.

The first approach has a great advantage of DC-coupling for the readout circuit. The second one needs AC-coupling and brings additional nuisances for high loads and long pulses. HVSys company[22] introduced power (bias) systems of detectors whose

[22] HVSys Company. Multi-channel biasing of SiPM, APD and Si-detectors, 2013.

architecture is aimed at low cost (≈ (20 − 30)$/ch) along with absolute sufficiency of their characteristics.

1. System modules serving up to 127 biasing cells (Fig. 16).The system module includes a power supply and microcontroller. It is connected to the mains, and through the communication line is connected to the host computer. Devices constructed as a desk-top design are housed in plastic cases or as a module in the standard of EUROMEKHANICS-6U 20 mm width.
2. A system bus that connects system modules to high-voltage cells. The system bus is made of a flat cable containing 10 lines located with a step 1.27 mm (0.050”) and IDC connectors.
3. Multichannel cells generating high voltage for detectors biasing. They are made as a small size box or printed circuit board incorporating a connector for connection to the system bus and an output connector to the detector.

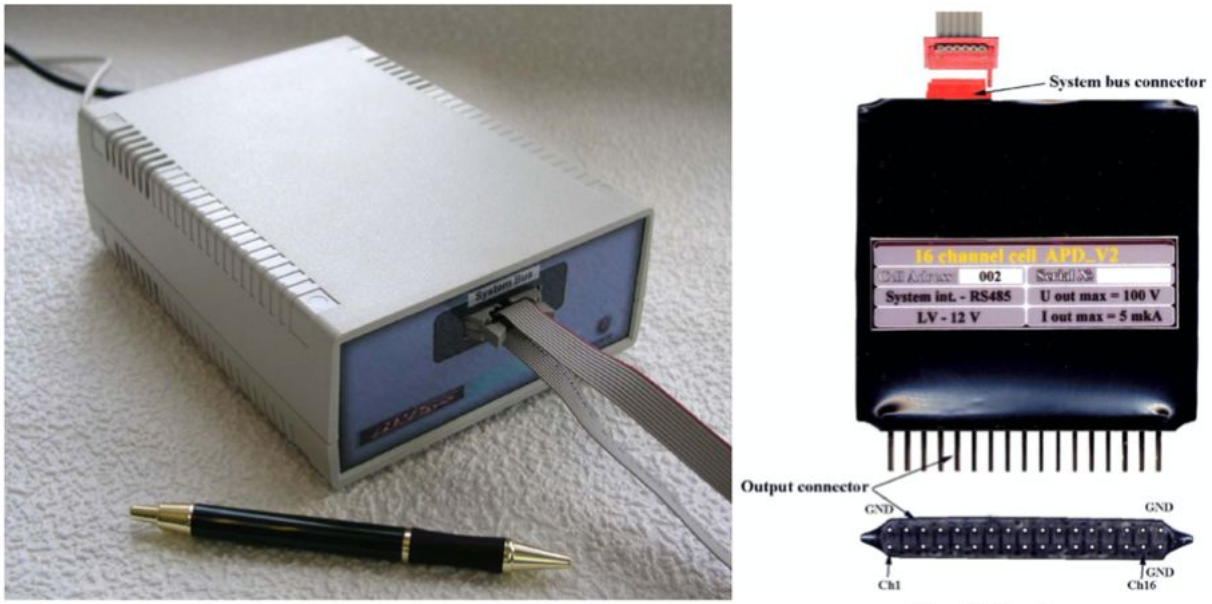

a) - HV unit b) - HV cell

Figure 16. SiPM power supply HV-sys company.

Following the second approach Fig. 15 (right) we develop a prototype by using 16 channel Digital-to-Analog Converters (DAC) which can produce voltage up to 40V (Texas Instruments DAC81416), see. Fig. 17. All 16 channels share a common current of 25 mA. Each channel supplies a single SiPM array with adjustable voltage within 16 (or 12) bits of dynamic range (±1V, ±2.5V, ±5V, ±10V,±20V, 40V). On another side we supply all SiPM with single voltage in order to add bias to SiPM operation point. Each of DAC is controlled by a micro-PC via SPI interface. Using this schematics we are able to control common current and cannot monitor each array individually. Main advantage of such schematics is a very low cost ≈ (5 − 10)$/ch.

http://hvsys. ru/images/data/news/7_small_1368803029.pdf

a) - Custom made HV unit by JINR

b) - DAC81416EVM by TI

Figure 17. Modules prototype of SiPM power supply based on Texas Instruments DAC.

We also develop a slow control software prototype which allows adjusting voltage at each DAC pin. This software is split by two parts. First is a demon (resident program) which continuously queries DAC and reads/puts parameters into MySQL database. Second is written on Java-script and presents parameters given in the database. It is installed on Apache server and could be accessible from everywhere via internet browser. The software GUI is shown in Fig. 18.

Figure 18. Software GUI for the JINR power supply prototype.

3.5.3 Mass characterization of SiPM

Another important task which will be handled by the JINR group is a need to verify all SiPMs parameters to reduce possible nuisances affecting energy resolution like: different breakdown voltage, PDE, Gain, cross-talks, etc.

3.5.3.1 Wafer level

Modern semiconductor technologies are well-developed allowing to produce SiPMs with high yield and with very narrow parameter spread. Hence the distribution of their characteristics on the wafer is rather small. Testing a grab sample of a few dies on the wafer at different points allows extrapolating the performance of sensors on the entire wafer. A good correlation of parameters with the SiPM bias voltage can be maintained within the same technological process. The simple and robust way to characterize SiPMs is to measure their IV, CV-curves by an automatic probe station done by a vendor. The method could be applied for individual characterization of SiPM at the wafer level in terms of similarity of breakdown voltage before array production. A similar voltage allows operating the whole SiPM array by applying voltage from a single source. This can help to reduce the number of voltage channels and make SiPM bias robust and cheap. To illustrate the idea of IV-curves (Fig. 19) we present measurements of a SiPM array[23].

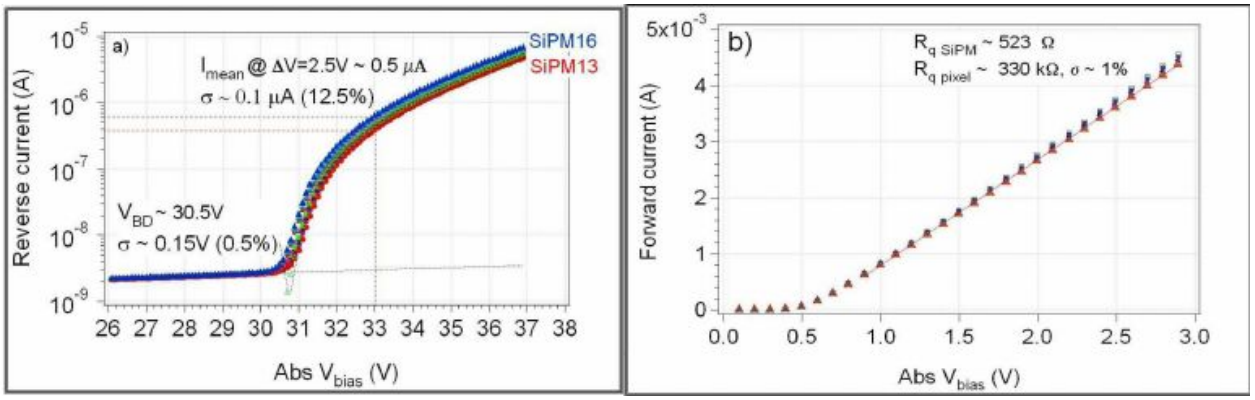

Figure 19. Reverse (left) and forward (right) IV-curves of 16 SiPM elements[23].

Measuring the IV-curve in forward biasing allows to probe the average quenching resistance. Meanwhile the reverse IV-curve denotes breakdown voltage and hence shows the operating voltage range. To find the breakdown voltage one can use the Inverse Logarithmic Derivative test[24]:

$$ILD(V) = \left(\frac{d\ln[I(V)]}{dV}\right)^{-1} = \left(\frac{1}{I}\cdot\frac{dI(V)}{dV}\right)^{-1}$$

Finding the minimum of ILD(V) returns the breakdown voltage Vbd. Another approach which demonstrates very robust determination of the voltage is to apply

[23] N. Dinu et al. Characteristics of a prototype matrix of Silicon PhotoMultipliers (SiPM). JINST, 4:P03016, 2009.

[24] V. Chmill, E. Garutti, R. Klanner, M. Nitschke, and J. Schwandt. Study of the breakdown voltage of SiPMs. Nucl. Instrum. Meth., A845:56–59, 2017.

quadratic fit on the inverse IV- curve[25].

After the wafer cutting and die packaging a sample batch of SiPMs is precisely studied by the standard methods. Matching IV-curves to measured parameters allow to certify a whole batch. To meet all experiment requirements it is advantageous to stay in contact with the producer in order to specify needs and methods of SiPM testing.

3.5.3.2 Array level

In total, we have to test about 4500 SiPM arrays. The first step is a visual check of resin (epoxy) surface quality for dust and bubbles. The second step is to simultaneously test 16 arrays which are put on a large testing PCB. Each array is supplied by an individual voltage source that allows precisely controlling current of each array. In dark conditions by using 16 self-stabilized LEDs[26] we can arrange the scan of 16 arrays simultaneously by using 16-channel ADC. Each LED is calibrated by means of a reference SiPM sitting next to each array as shown in Fig. 20a. The LEDs are placed above arrays and spot light on 1x1 cm. Large PCB is moved by two step-motors providing precise positioning of the LED beam with respect to each SiPM element on arrays as shown in Fig. 20b. To test all SiPMs on 16 arrays we have to provide 64 scans for 8x8 SiPM arrays. Each scan requires ~ 10^4 of acquisitions per SiPM which need about 10-20 minutes for full scan of 16 arrays. To test all arrays we need less than a month. This technique allows to characterize SiPM: PDE, Gain, Cross-talk, afterpulses and SPE. As cross-reference to wafer tests Breakdown voltage could be obtained from the pulsed current measurements by using an ADC.

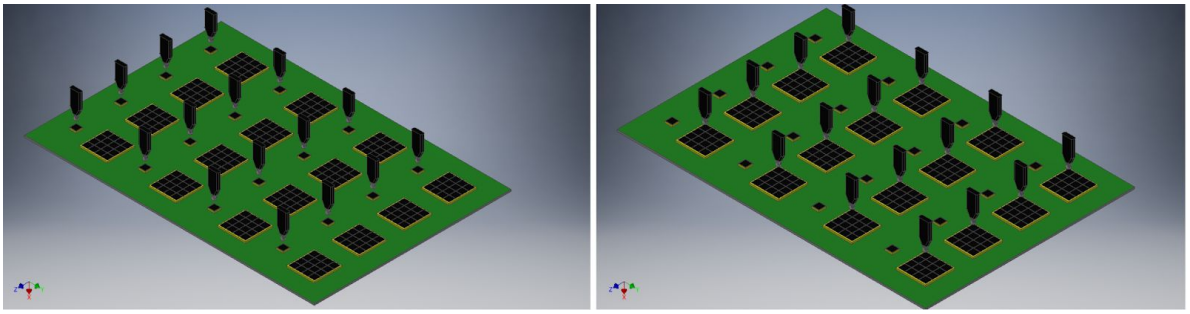

Figure 20. Array tests (schematic view). LEDs are in calibration mode (left), LEDs are in scanning mode (right).

3.5.3.3 R&D efforts of SiPM characterization

To study SiPM behavior at different operational temperatures, at DLNP, we build up a dedicated setup based on a Dewar vessel (Fig. 21). The vessel is used as a cryostat for Liquid Nitrogen (LN). Nitrogen vapor produces a gradient of temperature at different heights.

We can use this property to provide different temperatures in a broad range from room conditions down to LN environment. To provide a valid study we have to guarantee that light intensity is stable in time and with environmental changing. In our measurements we use the stabilized LED light source produced by HV-sys company.

---

[25] Claudio Piemonte, Roberto Battiston, Maurizio Boscardin, Gian-Franco Dalla Betta, A. Del Guerra, N. Dinu, Alberto Pozza, and Nicola Zorzi. Characterization of the first proto- types of silicon photomultiplier fabricated at itc-irst. Nuclear Science, IEEE Transactions on, 54:236 – 244, 03 2007.

[26] HVSys Company. Calibrated LED sources of light flashes, 2013. http://hvsys.ru/images/ data/news/5_small_1368802948.pdf

Preliminary, we observe the light variations which are delivered by a plastic optical fiber at level of about 10 % with temperature changing. It might be driven by changing optical properties between core and cladding. To cancel such a behavior we decided to stabilize temperature along the fiber length.

The cryostat vessel of 30 liters is filled with about 1/3 by Liquid Nitrogen (see Fig. 21a). An assembling of the light delivery system (see Fig. 21b) with SiPM is moving along the cryostat depth. Light delivery system is a copper pipe screens optical fiber bundle which is placed inside from temperature changing. We send light through the central fiber. Other fibers were used as a monitoring system to check the light stability with temperature changing. The pipe is wound by heating cable with feedback provided by a thermal sensor which is placed inside the pipe. The assembly is thermally insulated outside. We placed a reflection dice in front of the fiber bundle and checked the light stability with high light intensity. High enough to use silicon PIN-photodiode to monitor reflected light. Our measurements presented stability at level of 1%.

We replaced the reflection dice with a SiPM and stuck it with thermal grease to aluminum substrate (bed) with an embedded thermosensor on its backside. Temperature stability is guaranteed with precision < 1 °C.

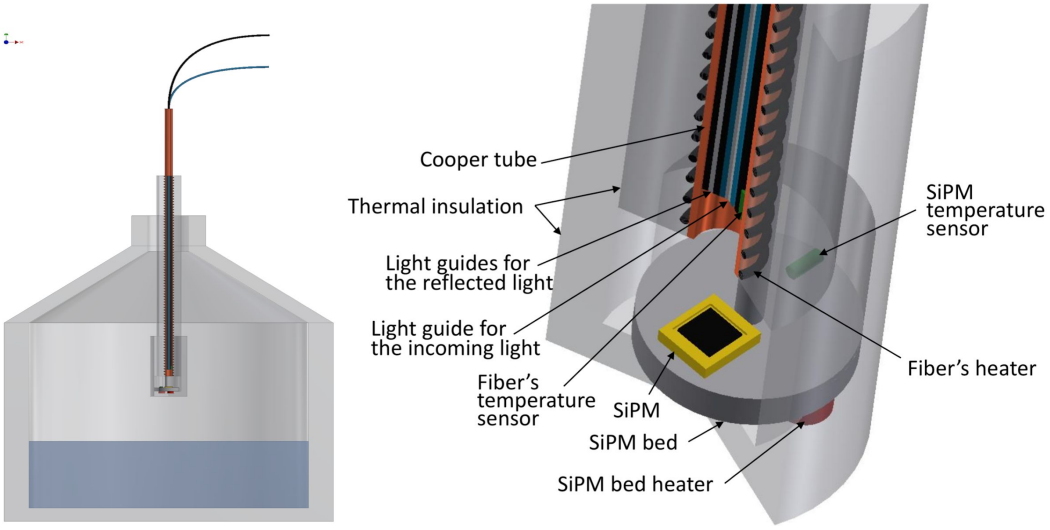

Figure 21. Setup for studying SiPM parameters behavior at low temperatures. The Assembly dip in the Dewar vessel, Nitrogen vapor (left). Assembly of the light delivery system with SiPM (right).

We are going to test a few SiPM samples in order to choose a candidate for the TAO and then make mass tests. During mass tests we may also sample SiPMs and characterize them by using the stand.

We are also planning to test a batch of SiPM for long-term operation at -50 °C.

3.6 PMT test equipment and status

3.6.1 Scanning stations

The JUNO setup will use about 20'000 of Large Photocathode 20" PhotoMultiplier Tubes (PMT), which read out the sphere barrel filled with 20 kton of a liquid scintillator. One of the experiment's largest challenges is to achieve the unique energy resolution of ~3% at 1 MeV and to provide very stable and reliable operation during the whole life of the experiment which dictates very crucial requirements for the PMTs. Hamamatsu (Japan) R12860 20'' PMT and NNVT (China) 20'' MCP-PMT were chosen for the JUNO experiment. The JUNO collaboration approved a list of requirements for the PMT acceptance. These are: PDE (Photon Detection Efficiency)>24% (@425 nm), Gain ~10^7, Dark rate<50 kHz, Peak-to-Valley ratio >2.5 and other. An important parameter is the inhomogeneity of the PDE over photocathode, which should be less than 15%. The latter measurement needs a scanning device to obtain parameters of the PMT differentially.

The group at JINR constructed and commissioned a dark room with the scanning station at JINR and two dark rooms with two scanning stations on the PMT testing site in China. The differential and integral characteristics of a large PMT strongly depend on the direction and magnitude of the Earth's magnetic field. The darkrooms allow measurements in magnetic fields of different magnitudes (including full magnetic field compensation) by using Helmholtz coils.

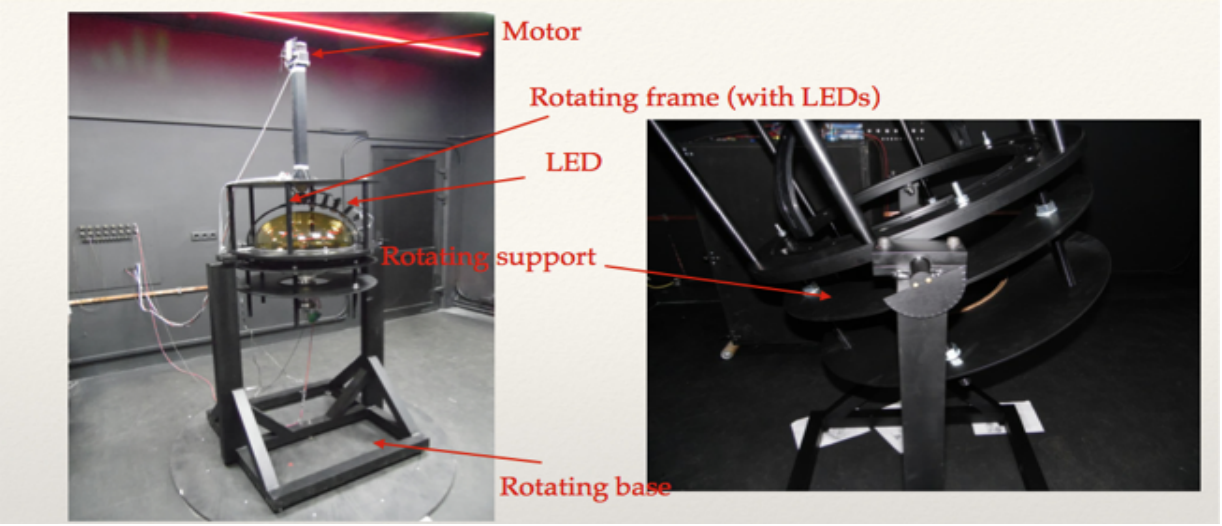

Figure 22. Scanning station in the dark room at JINR.

The core of the scanning station is a rotating frame with 7 stabilized compact pulsed light generators that are placed with different zenith angles. Frame is rotated by the step motor and covers all 360-deg azimuth angles. A support system that holds PMT allows rotations in different space positions in order to put the PMT in different orientations with respect to the magnetic field provided by the dark room. It allows testing individual PMTs in all relevant aspects by scanning the photocathode and to understand the performance of a PMT in depth and to identify any potential problem.

To satisfy the requirements, the system is based on FPGA that provides multi-trigger signals for LEDs, ADC board (DRS-4) and is used as a scalar that replaces expensive commercial electronics. Our team designs and produces fast amplifiers with gain of 10 for more reliable PMT's signal measurement.

A testing method is based on very low-intensity light flashes (~ 1 ph.e) to obtain gain, average number of photoelectrons and other parameters[27]. By using a calibrated light source we can characterize photon detection efficiency of the tested PMT.

The source of light is a know-how of the HVSYS company[28]. It is an LED stabilized pulse source compact device of 80x22x11 mm in size, implemented in a single package. The stabilization is provided by a PIN-photodiode that monitors the LED light. The PIN feedback is made up of ADC digitizing PIN signal and DAC controlling the LED amplitude. Both of them are embedded in a small chip of the microcontroller. A calibration of the light source is done by the calibrated photosensor (small PMT with known PDE).

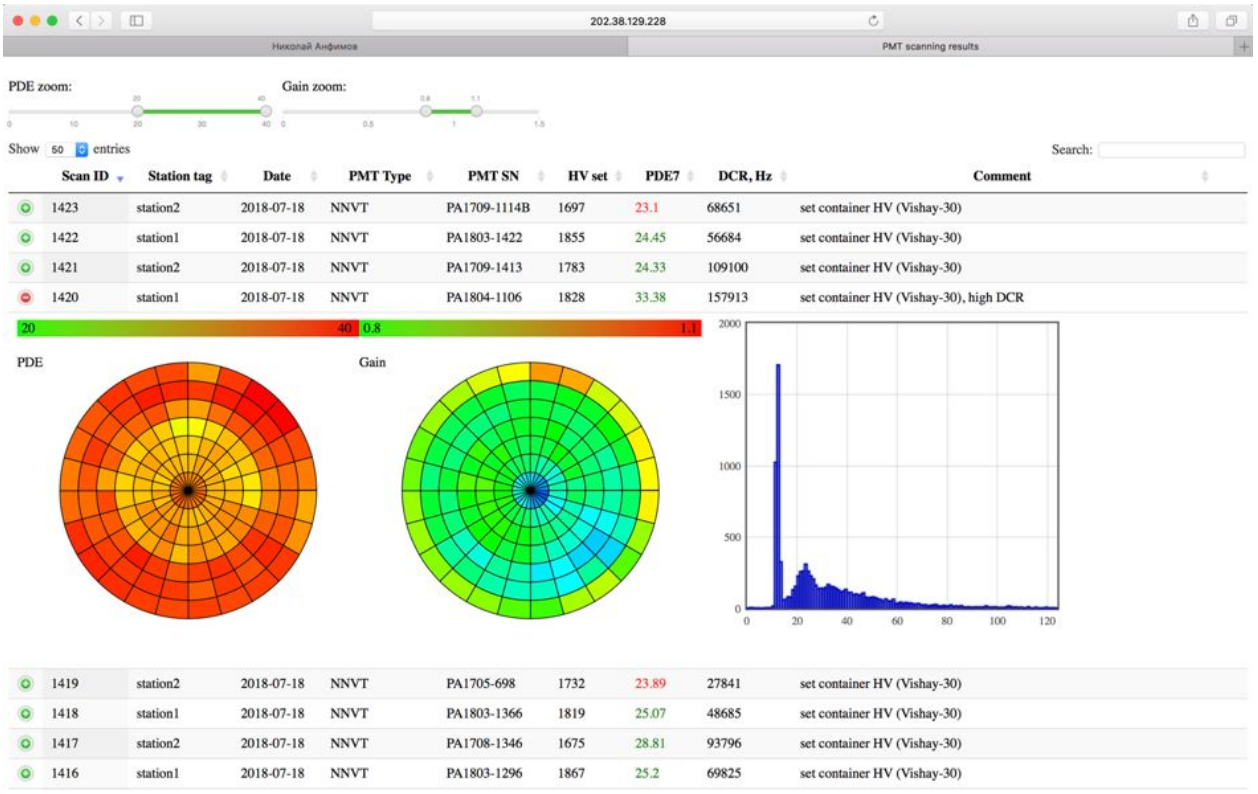

Figure 23. Web interface of the PMT scanning station's Database.

The JINR group developed the software based on modern IT-technologies for controlling the scanning station, acquiring, processing and storing the data (see Fig. 23) coming from the station.

Users or operators can easily access the data and visually check out consistency of the measurements.

Two scanning stations were prepared for on-site installation in China and about 2500 PMTs have been tested. Each of the scanning stations is equipped with its own dark room. So far, we have built 3 scanning stations. One of those stations stays at JINR to study potential problems which might happen in China.

The scanning station is a precise instrument that is complementary to the mass testing (container) system. It provides a cross-checking of suspicious PMTs that failed the simple tests.

---

[27] Optimization of the light intensity for Photodetector calibration. By N. Anfimov, A. Rybnikov, A. Sotnikov. [arXiv:1802.05437 [physics.ins-det]]. 10.1016/j.nima.2019.05.070. Nucl.Instrum.Meth. A939 (2019) 61-65.

[28] http://www.hvsys.ru

3.6.2 Containers and mass testing

The JUNO Collaboration is preparing equipment (German group) for the mass tests of all PMTs using 4 dedicated containers (Fig. 24). Two containers consist of 36 drawers. Another two have 32 drawers and intended for long-term stability and potted PMT with 1F3 electronics tests. Each drawer will test a single PMT. This approach allows us to test 72 PMTs in parallel. The basic measurement in the container will be the PMT response during illumination of its photocathode by the uniform light of a small intensity. All of the 20000 PMTs will undergo the container test.

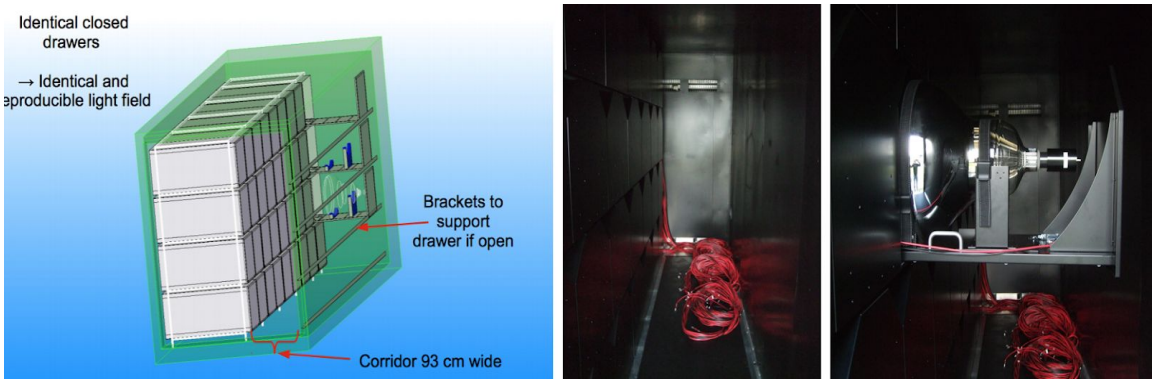

Figure 24. The Container. General view (left), corridor (middle), PMT layout in the drawer (right).

The light field inside the drawer is provided by the HVSYS LED light source. Four containers require about 150 of light sources. One of the JINR responsibilities was to supply collaboration with all the light sources used in the containers. Light source is placed in a special holder and light is spread by a PTFE-diffuser plate. We got the real part of the system from Germany to check light field distribution inside the drawer. Having a 3D-printer in our lab we printed out an arc that mimics a large PMT shape. The arc has holes to attach small PMT. By moving small PMT to different positions we can evaluate the light field on the real PMT surface in the drawer.

Another important task is to match integral and differential results together. For that reason the dark room has been equipped with optical fiber that guided light from a picosecond LASER. The fiber is placed far from large PMT in order to spill the light homogeneously to the PMT surface. Another option is to apply fiber to the drawer light diffuser to check the consistency with the LED light. The PMT itself is securely held in the scanning station support without the cap that drives the arc with LED. The technique allows to measure all the main PMT parameters as: gain, PDE, P/V, TTS by illuminating the whole PMT surface.

3.6.3 Container for long term testing

The main goal is to identify any potential problems with PMT during long term operation: variation of the characteristics, PDE degradation, operation failures. One of the containers (the third) was equipped for performing the long term PMT testing. With standard usage of self-stabilized LEDs operating in a low-intensity flash mode, we put another two LEDs (see Fig. 25, left): first is operating to produce high light intensity pulses to stress out a PMT by mimicking muon signals, second is in continuous light mode to reproduce uniform extra stress by single electron signals to speed up the PMT aging. We also put white PTFE film to reflect light back in order to guide it through the

front diffuser (Fig. 25, right).

We equipped all the 32 drawers both with self-stabilized LEDs in low-intensity flash mode and LEDs producing continuous light. And we equipped 24 drawer boxes with the LEDs producing high light intensity pulses (Fig. 26)

Our group also developed and produced 32 channel counter/scaler based on FPGA to monitor the dark rate of the PMTs. We also purchase 32 channel HV-unit produced by HV-sys company.

Dedicated software for continuous and automated data taking was developed. Currently, we have set up all the equipment and are taking data since Nov 2019.

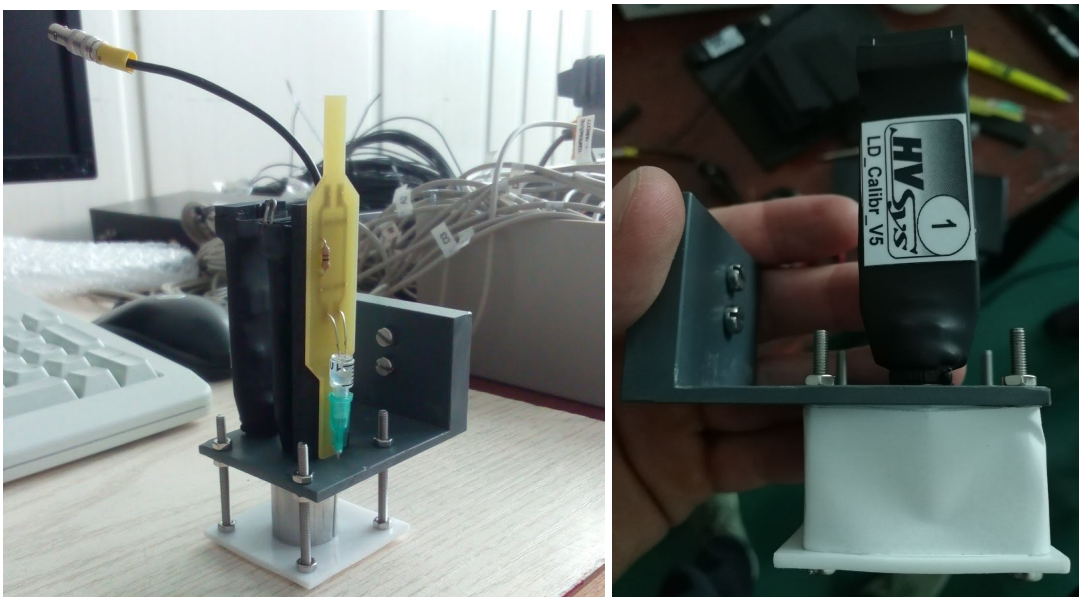

Figure 25. Light system for the Long-term PMT testing. LEDs setup inside the container.

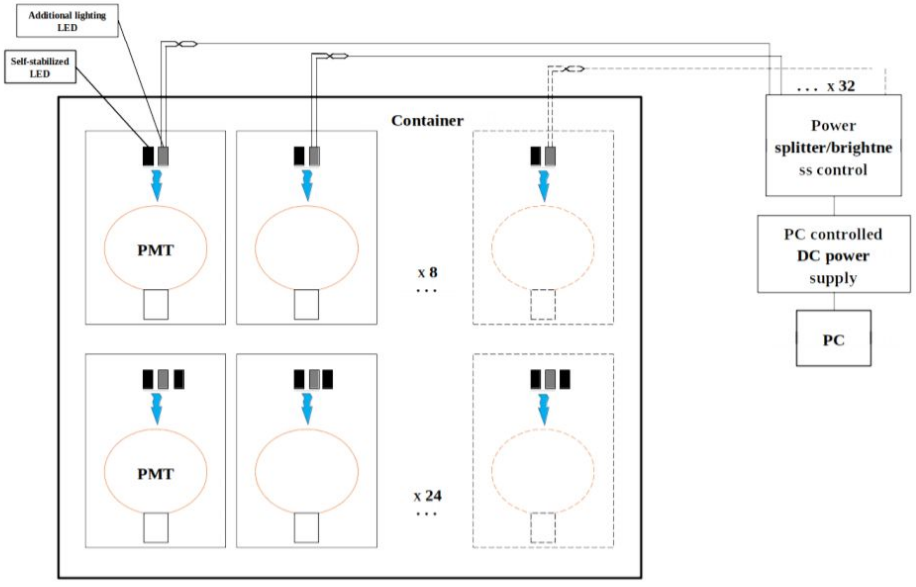

Figure 26. Block-scheme of the Long-term PMT testing.

3.6.4 Performance and Results

Currently, about 3900 scans were performed and about 2500 PMTs were tested: 350 Hamamatsu and 2200 NNVTs. Some of the scans are repetition for reference and monitoring PMTs, some are a set for the magnetic studies (5-6 scans per PMT).

To match results between the scanning system and the container we evaluate integral PDE by summing differential values of the PDE times their weights. Each weight is the sector relative area on the PMT surface. The joint analysis for NNVT and HQE NNVT tubes are shown in Fig. 27.

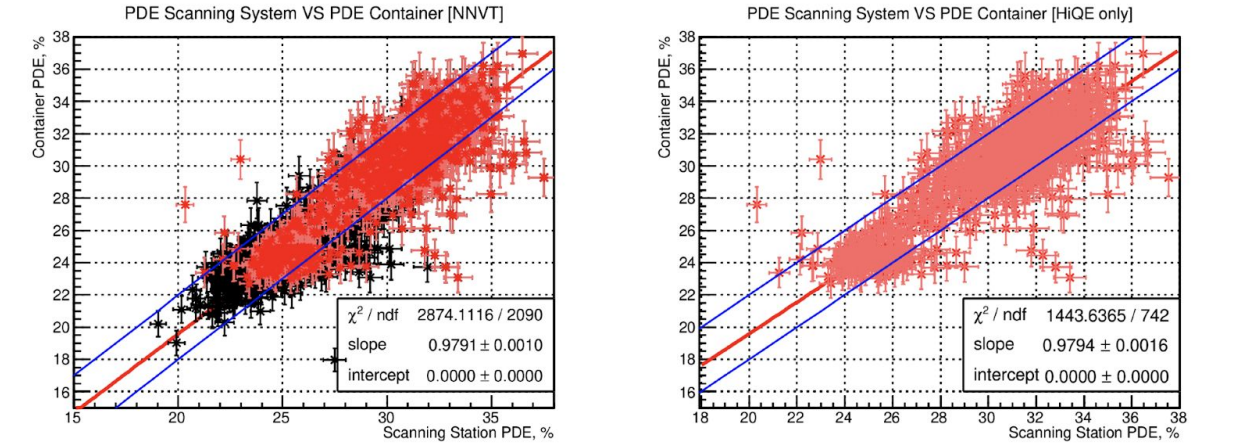

Figure 27. Comparison of the PDE probing by two systems: scanning station and container.

The main intention of the scanning station is to characterize the non-uniformity of the PDE. We measure it as a square root of a relative weighted variance to the weighted average. The results are shown in Fig. 28. The numbers underneath each plot indicate a batch of scanned phototubes of different kinds. In the brackets are the numbers of failed tubes which have non-uniformity higher than 15%.

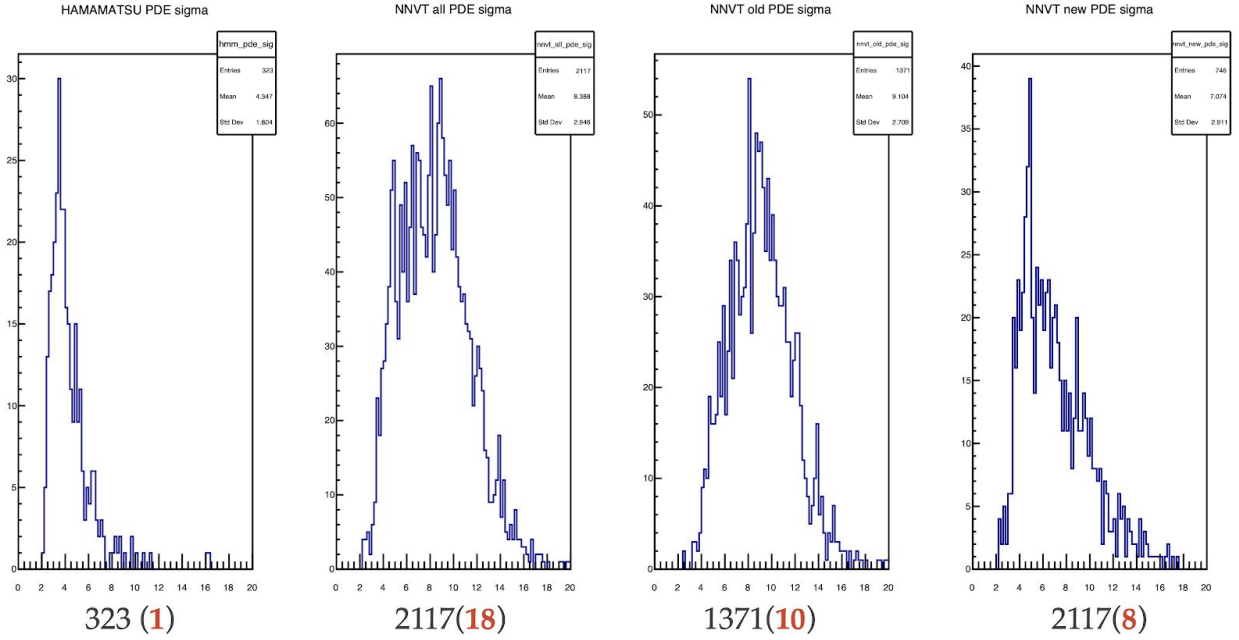

Figure 28. Non-uniformity distribution for scanned PMTs.

The JUNO collaboration specified the requirement for a PMT to be insensitive to

the magnetic field up to 1/10 to EMF (5 μT). We use one of the scanning stations to scan PMTs in different values of the magnetic field in range from 0 to 20 μT with a step of 5 μT. Most of the probed tubes are applicable up to 15 μT which is 3 times larger to the required one (see Fig. 29). It is interesting to note that the gain behavior differs for the dynode (Hamamatsu) - growing and MCP (NNVT) tubes - decaying.

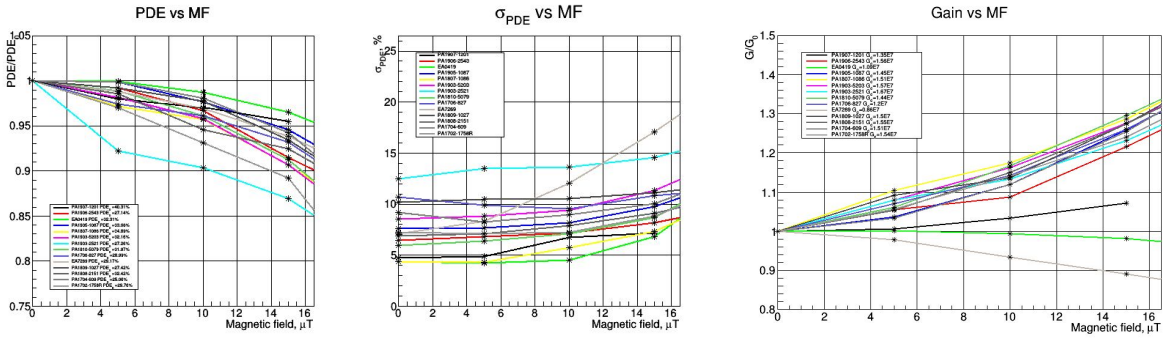

Figure 29. PMT operation vs magnetic field: PDE, σPDE and Gain.

We are also involved in the analysis data coming from two containers. 16643 tubes have been tested for 4 of April 2020: 5182 Hamamatsu tubes and 11461 NNVT tubes. 5007 and 9207 of them had passed the test respectively, and 88 and 475 were rejected. The potted PMTs pass the test again. 3110 tubes were tested after the potting. About 30 potted tubes have been scanned. We are aiming to learn the PMT operation after potting. If it is similar to bare PMTs we are going to proceed with sample tests to control parameters otherwise we have to retest all potted tubes. Similar situation with 1F3. The plan is to sample tubes and test them with 1F3 to check out the operation consistency.

3.7 Protection of PMT against Earth Magnetic Field

3.7.1 Coil compensation scheme for JUNO CD and Veto

Insensitivity from the Earth Magnetic Field (EMF) is a necessary request of any experiment, where the PMTs are used for the photodetection. The JUNO collaboration specified the requirement for a PMT itself to be insensitive to the magnetic field up to 1/10 of EMF (~5 μT). Correspondingly, the EMF at the JUNO PMT positions should be decreased down to less than this value.

There are two general approaches to achieve this: use coils to compensate for EMF in the volume or shield it using materials with high magnetic permeability. Early calculations performed by the JINR experts have shown that the first approach is more practical for JUNO and a special coils configuration, producing horizontal and vertical compensating fields (Fig. 30), was later adapted by the Collaboration[29].

[29] J.Songwadhana et al., "Earth Magnetic Field Shielding for JUNO", JUNO Document 5149-v3 (to be published).

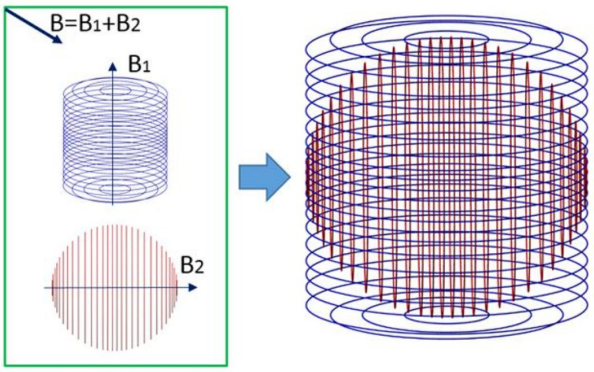

Figure 30. The schematic diagram of JUNO active geomagnetic shielding coils.

It was shown by the calculations (which were cross checked with the prototype testing) that the JUNO requirements are well satisfied for all of the PMT positions at the CD (Fig.31, left) and Water Cherenkov Veto (Fig.31, right).

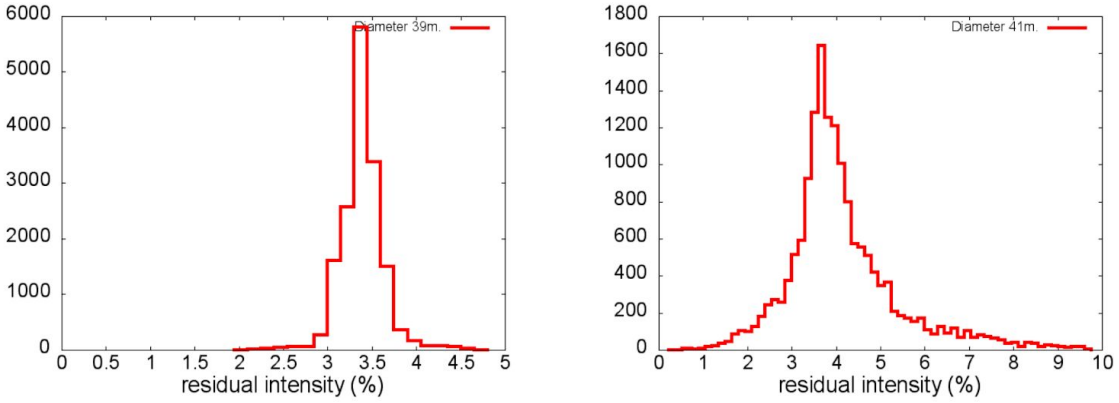

Figure 31. Residual Intensity of magnetic field at the PMT positions of CD (left) and Water Cherenkov Veto (right).

In addition, the JINR group has studied a backup solution of PMT individual shielding using modern magnetic materials. This option is applied now to the PMTs of a special 20t Liquid Scintillator (LS) detector - OSIRIS, which was proposed to monitor the quality of the JUNO 20 kt of LS production during 6 months of the JUNO CD filling.

3.7.2 PMT protection against Earth Magnetic Field for OSIRIS

Characteristics of large PMTs (20”) to be used in OSIRIS degrade in the presence of the weak magnetic field of the Earth of about 50 μT. Hence, for the non-disturbed PMT operation one needs either compensate the magnetic field (as it is envisaged for the main JUNO detector) or screening of the Earth magnetic field with high magnetic permeability materials. The magnetic shielding of the PMTs will screen the PMTs from the Earth Magnetic Field (EMF).

The EMF screen (EMFS) developed at the DLNP consists of two elements: the main cone and the additional cylindrical part. The magnetic properties of the design are defined by the use of the amorphous metal (or metal glass, metglas) tape АМАГ-170 produced in Russia (Borovichi, Novgorod region) with extremely high magnetic permeability reaching 10^6. The very high magnetic permeability of the material is a milestone of the design, as it allows to reduce the total weight of the material in the

vicinity to the sensitive region of the OSIRIS detector. An important property of the metglas in comparison to more common permalloys is stability of its properties, the material doesn't need annealing after the processing.

The both components of the EMFS are manufactured using the composite materials (cheaper fiberglass and/or more expensive carbon fiber). The metglas tape АМАГ-170 (30 um thickness and 30 mm wide) is placed between the layers of the composite material in a way to guarantee the average thickness of the material of 0.2 mm, the total weight of the metglas tape for one screen is about 1.5 kg. The uniformity of the tape placement is not critical, the screening properties are defined mainly by the total mass of the used material.

Two variants of the EMFSs will be produced: for the muon veto (12 pieces) and for the main detector (64 pieces). The EMFSs of the muon veto PMTs will be manufactured using less expensive composite material on the base of fiberglass. The material is too radioactive to be used for the main detector PMTs mainly because of the high content of the potassium in fiberglass and gelcoat, and more expensive composite material on the base of carbon fiber will be used. Mass of materials used for the production of both variants of EMFSs is summarized in Tab. 3 and Tab. 4.

The fiberglass needs protective covering against water to prevent degradation of the mechanical properties of the material, the black gelcoat is used for this purpose. The carbon fiber material is naturally black and water resistant, it doesn't need additional covering. The black colour of the surfaces exclude undesired reflections from surfaces. In the additional element the inner surface is covered with white reflecting coating. According to MC optical simulations the reflecting coating will improve light collection at the PMT photocathode.

The layer of the magnetic shielding is accompanied by an aluminum layer providing additional screen for the rf-noise.

The results of the test of the magnetic screen properties are presented in Fig. 32. The most critical component of the magnetic field is the one perpendicular to the axis Z (axis of symmetry), the field along this direction has the most destructive influence on the PMT characteristics. As can be seen in Fig. 32 the EMFS significantly reduces magnetic field in this direction. The reduction factor varies from 3 to 12 inside the PMT bulb and the large fraction of the PMT volume is well-protected against this component of the EMF. The coefficient of the magnetic field reduction along the Z axis is significantly lower, its maximum value at the center of the PMT is 2. Nevertheless, this reduction is found acceptable for PMT operation due to the low sensitivity of PMT to Z component of the magnetic field. We checked the alternative design of the construction with the use of the mu-metal grid in place of the additional element. This variant provides better screening of the Z-axis field of about 2.5 compared to factor 2 of the main design, but suffers from the "shadow effect" of the opaque grid: the loss of light is about 6% for the 50 mm step grid made of mu-metal wire 1.5 mm in diameter. The loss of light and complexity of post-production processing (annealing of the construction needs a large oven and special covering is needed to protect mu-metal from corrosion in pure water) makes the construction much less attractive.

The OSIRIS detector will be used for the monitoring of ultra-low levels of radioactivity in the liquid scintillator of JUNO before filling. Hence, the materials of the detector should contain very low amounts of the natural radioactive elements from U/Th chains and potassium. The abundance of radioactive ^{40}K in natural potassium is 1.17×10^{-4}. The total flux of gammas from radioactive impurities in construction materials should not exceed the corresponding flux from PMTs, providing the most powerful

irreducible source of radioactivity (radioactive impurities are contained mainly in the PMTs glass). All materials to be used in EMFSs were tested on the content of the radioactive impurities, the results are summarized in Tab. 5 and Tab. 6.

The manufacturer of the components of EMFSs is LLC “Hydromania” (Minsk) All the operations are performed in the devoted isolated room, the efforts are taken to exclude the deposit of dust on the surfaces. The ready EMFSs are washed and packed in polyethylene film to exclude the contact with the atmospheric radon and hence the accumulation of the radon decay products on the surfaces. The shield will be additionally cleaned using special liquids and ultrapure water before the installation in the OSIRIS.

Status of production (as of April, 2020): two sets of templates for EMFS production are prepared; three fiberglass prototypes of the main part and two additional elements are produced. One prototype is on its way to Germany for the mechanical compatibility tests. Another prototype is used for the tests with PMT. The contract for the production of 12 EMFSs for the muon veto is being signed. The production will be started as soon as mechanical compatibility is confirmed at German side. The contract for 64 EMFSs for the main detector is being prepared.

Material	Main element, kg	Additional element, kg	Total, kg
Fiberglass	0,8	0,36	1,16
Epoxy	1,018	0,458	1,476
Gelcoat, black	1,4	0,35	1,75
Gelcoat, white	-	0,35	0,35
Tape АМАГ-170	1,015	0,55	1,565
Al foil	0,06	0,03	0,09
Cu foil	0,05	0,03	0,08
Total	4,343	2,128	6,471

Table 3. Weight of materials used for production of the first variant of EMFS (the prototype and screen and the base of fiberglass with black gelcoat covering).

Material	Main element, kg	Additional element, kg	Total, kg
Carbon fiber	0,57	0,25	0,82
Epoxy	0,82	0,37	1,19
Gelcoat, white	-	0,35	0,35

Tape АМАГ-170	1,015	0,55	1,565
Al foil	0,06	0,03	0,09
Cu foil	0,05	0,03	0,08
Total	2,515	1,580	4,095

Table 4. Weight of materials used for production of the second variant of EMFS (screen on the base of carbon fiber).

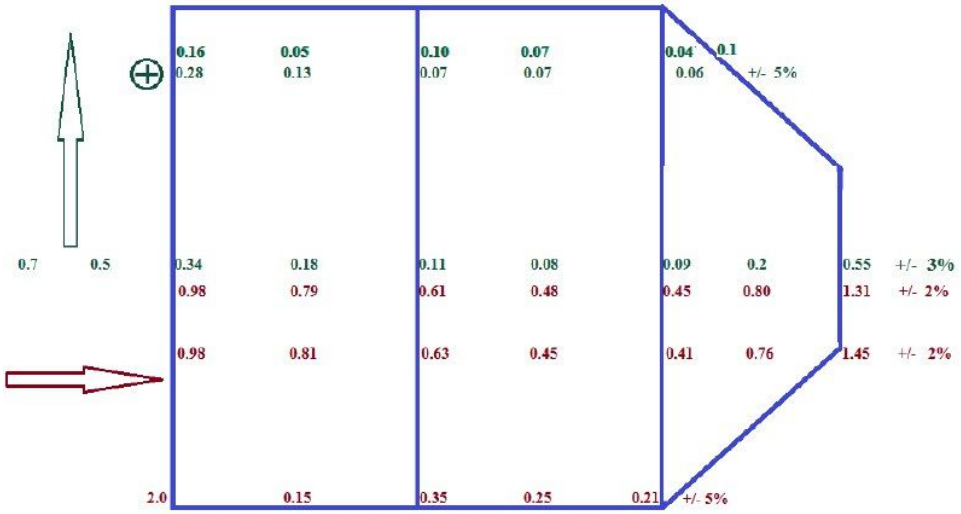

Figure 32. The reduction of the weak magnetic field along two directions: along the axis of PMT or Z-axis (red colour) and perpendicular to the PMT symmetry axis (green colour). The values for the field reduction near the walls are shown for two directions: along the applied field and in the perpendicular direction (from the "observer"), the former values correspond to the row marked with cross sign.

Material	U ppb	Th ppb	K ppm	m(U) μg	m(Th) μg	m(^{40}K) μg
Fiberglass	5833	<3	1460	6770	<4	198
Epoxy	<0,1	0.9	0,78	<0,15	1,3	0,13
Gelcoat, black	<3	<0,3	177	<5,3	<0,5	36
Gelcoat, white	7	7	4,33	2,5	2,5	0,2
Tape АМАГ-170	3	<5	0,84	4,7	<7,8	0,154
Cu foil	0,3	0,2	0,127	<0,024	<0,016	<0,001

Al foil	170	26	0,96	15,3	2,4	<0.01
Total				6798	<18	234
PMT glass	400	400	60	3600	3600	63

Table 5. The abundance of radioactive impurities and its total content in the elements of the fiberglass based construction. The last row contains the corresponding values for the PMT glass (9 kg) and is provided for comparison. Certification of all material was performed by LLC “ARMOLED” («АРМОЛЕД») (Moscow) under contract with JINR.

Material	U ppb	Th ppb	K ppm	m(U) μg	m(Th) μg	m(^{40}K) μg
Carbon fiber	3	<5	0,84	0,25	<4,9	1,4
Epoxy	<0,1	0.9	0,78	<0,12	0,11	0,1
Gelcoat, white	7	7	4,33	2,5	2,5	0,2
Tape АМАГ-170	3	<5	0,84	4,7	<7,8	0,154
Cu foil	0,3	0,2	0,127	<0,024	<0,016	<0,001
Al foil	170	26	0,96	15,3	2,4	<0.01
Total				22,8	<18	1,9
PMT glass	400	400	60	3600	3600	63

Table 6. The abundance of radioactive impurities and its total content in the elements of the carbon fiber based construction. The last row contains the corresponding values for the PMT glass (9 kg) and is provided for comparison. Certification of all material was performed by LLC “ARMOLED” (ООО «АРМОЛЕД») (Moscow) under contract with JINR.

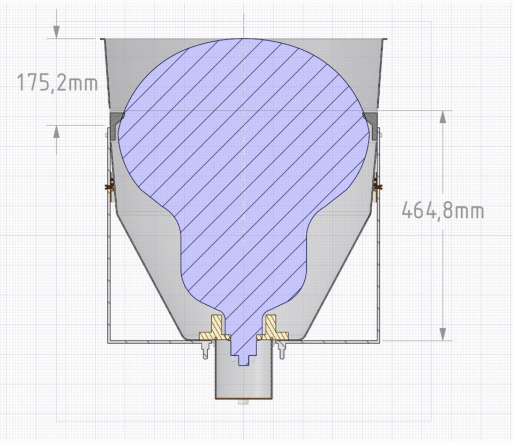

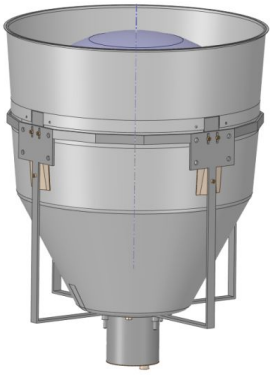

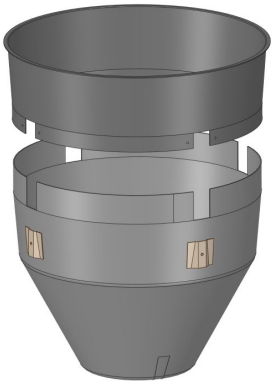

Figure 33. EMFS of the PMT shown together with PMT and elements of construction. The main element of the EMFS is placed below the bulb “equator”, the additional element is above the “equator”.

Figure 34. The main element of the EMFS (photo of the prototype).

Figure 35. The additional element of the EMFS. In the second photo one can see the electrical contact of the rf-screen. The main element has the same contact too.

3.8 R&D of liquid scintillator. Tellurium doping

The long-term use of the JUNO detector suggests its redirection to search for neutrinoless double beta decay. One of the ways of such transformation is doping the liquid scintillator with tellurium (130Te), which has practical advantages for studying this process.

In the SNO+ project, it was planned to develop a liquid scintillator based on linear alkylbenzene with the addition of 2.5-diphenyloxazole (2 g/l) with a tellurium content of 0.3% by weight to search for neutrinoless double beta decay. To solve this problem, it was initially planned to use an aqueous solution of telluric acid and a surfactant[30]. However a more advanced approach was developed for loading tellurium into a liquid scintillator based on synthesis a tellurium-butanediol complex. This approach allowed

[30] Andringa, S., et al. "Current status and future prospects of the SNO." *Advances in High Energy Physics* 2016 (2016).

achieving better optical properties and increasing the tellurium content to 0.5% by weight[31,32].

Our goal is to increase its rate and develop a liquid scintillator with a tellurium content of at least 1%.

[31] Biller, Steven, Szymon Manecki, and SNO+ collaboration. "A new technique to load 130Te in liquid scintillator for neutrinoless double beta decay experiments." *Journal of Physics: Conference Series*. Vol. 888. No. 1. IOP Publishing, 2017.

[32] Caden, Erica. "Status of the SNO+ Experiment." *Journal of Physics: Conference Series*. Vol. 1342. No. 1. IOP Publishing, 2020.

4 The staff

№	Name	Info	FTE 21	22	23	Tasks
1	N. Anfimov	staff	0.4	0.4	0.4	PMT testing group leader
2	T. Antoshkina	PhD student	1	1	1	PMT optics response simulation. Formulation of requirements for PMT testing quality
3	S. Biktemerova	PhD student	1	1	1	sensitivity estimation, detector simulation, data analysis
4	A. Bolshakova	staff	1	1	1	PMT data analysis
5	I. Butorov	engineer	0.5	0.5	0.5	Designing and technical work/ PMT testing, analysis
6	A. Chetverikov	engineer	0.3	0.3	0.3	Designing and technical work/ PMT testing
7	A. Chukanov	candidate	0.7	0.7	0.7	Reconstruction, data analysis
8	S. Dmitrievsky	candidate	0.5	0.5	0.5	Simulation and software development for TT
9	D. Dolzhikov	student	0.2	0.4	0.4	Selection and analysis
10	D. Fedoseev	engineer	0.3	0.3	0.3	Designing and technical work
11	M. Gonchar	PhD student	1	1	1	sensitivity estimation, detector simulation, data analysis
12	Yu. Gornushkin	candidate	0.5	0.5	0.5	The TT project coordination
13	M. Gromov	candidate	0.5	0.5	0.5	Analysis, SuperNOVA
14	V. Gromov	engineer	0.5	0.5	0.5	Software development for TT/TAO JUNO
15	D. Korablev	staff	0.6	0.6	0.5	software development for PMT testing and TT, Long term-stability, PMT testing, Analysis
16	A. Krasnoperov	candidate	0.3	0.3	0.3	Software development for TT JUNO
17	N. Kutovskiy	candidate	0.2	0.2	0.2	IT
18	K. Kuznetsova	engineer	0.3	0.3	0.3	SiPM testing, Analysis
19	Y. Malyshkin	candidate	0.5	0.5	0.5	Analysis, reconstruction
20	D. Naumov	doctor	0.5	0.6	0.7	project management. Reactor spectrum measurement. Oscillation analyses. Global analysis
21	E. Naumova	PhD student	1	1	1	Reactor spectrum measurement.
22	I. Nemchenok	candidate	0.5	0.5	0.5	Investigation of properties and stability of liquid scintillator
23	A. Olshevskiy	doctor	0.5	0.5	0.5	analysis preparation, HV and other JINR hardware activities coordination
24	A. Rybnikov	engineer	0.3	0.3	0.3	PMT testing, SiPM testing
25	A. Sadovsky	candidate	0.5	0.5	0.5	PMT HV R&D
26	D. Selivanov	student	0.2	0.2	0	Reconstruction

27	A. Selyunin	engineer	0.2	0.2	0.2	PMT testing
28	V. Sharov	engineer	0.5	0.5	0.5	PMT testing
29	A. Shaydurova	student	0.2	0.2	0	Neutrino oscillations in matter
30	V. Shutov	engineer	0.3	0.3	0.3	HV unit software and tests
31	O. Smirnov	candidate	0.5	0.5	0.8	PMTs magnetic shielding, energy resolution studies
32	S. Sokolov	engineer	0.5	0.5	0.5	Designing and technical work, PMT testing
33	A. Sotnikov	engineer	0.3	0.3	0.3	PMTs magnetic shielding, PMT tests
34	M. Strizh	student	0.2	0.2	0	reconstruction of neutrino directionality
35	V. Tchalyshev	candidate	0.5	0.5	0.5	SiPM testing, clean room support
36	K. Treskov	PhD student	1	1	1	sensitivity estimation, software development, data analysis
37	N. Tsegelnik	student	0.5	0.5	0.5	fitting software development
38	V. Zavadskyi	student	0.2	0.2	0.4	Oscillation Analysis
39	O. Zaykina	staff	1	1	1	Reconstruction
	Total FTE		**19.7**	**20.0**	**19.9**	
	People		**39**	**39**	**36**	
	FTE/person		**0.51**	**0.51**	**0.55**	

Table 7. JINR staff in JUNO and Daya Bay.

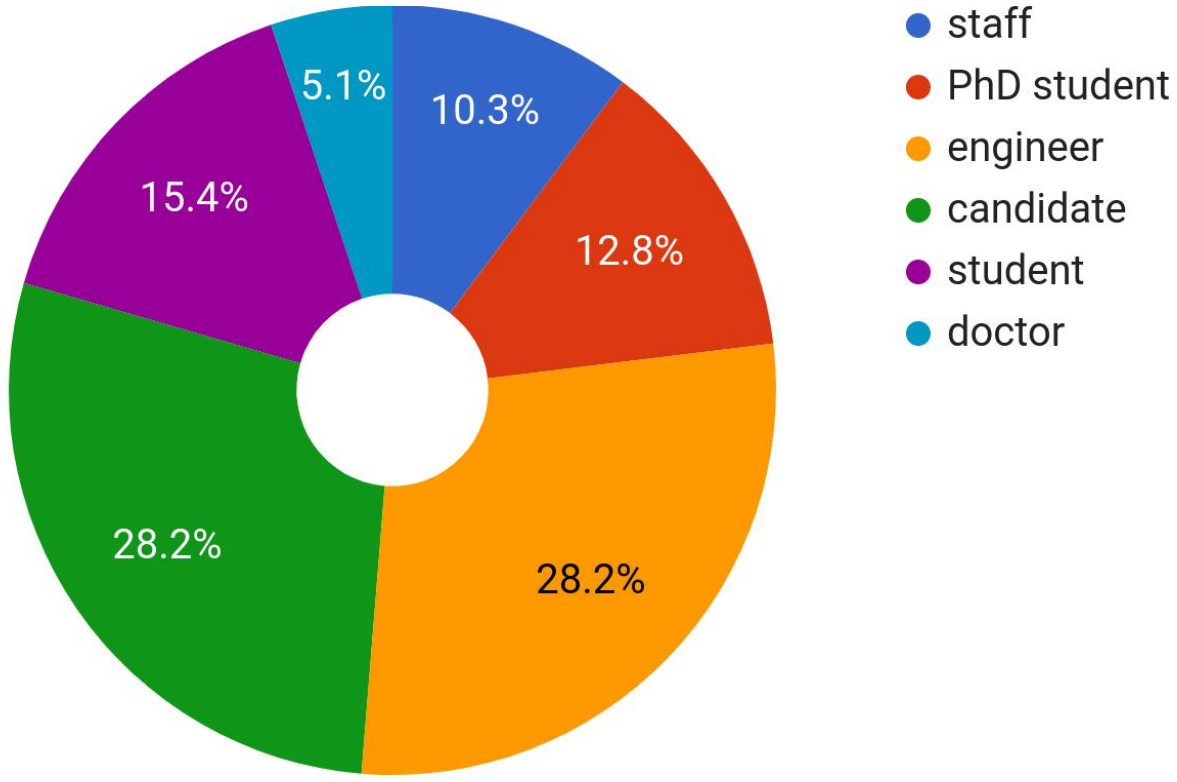

Figure 36. Staff status distribution.

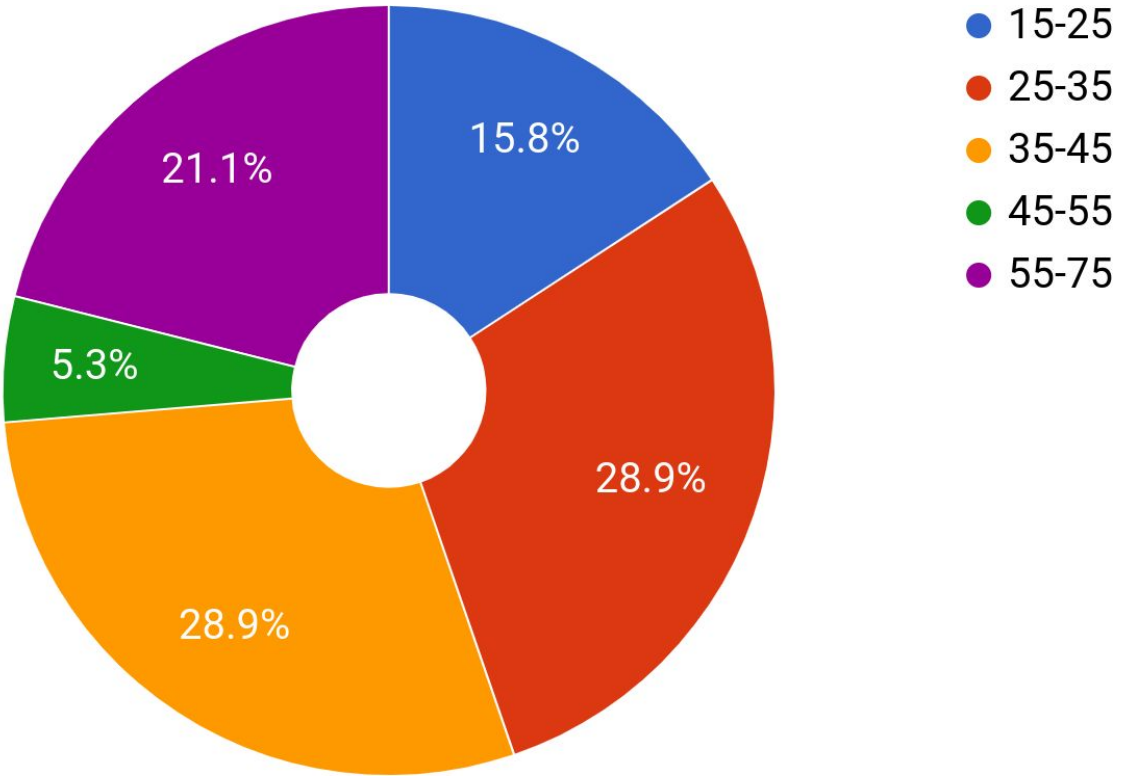

Figure 37. Staff age distribution.

5 SWOT analysis for the JUNO project

	Helpful	Harmful
Internal	**STRENGTHS** ● Neutrino hierarchy determination by method different from other experiments ● Precise oscillation parameters measurement ● Geo-neutrinos measurement ● Other neutrino physics (solar, atmospheric, etc.)	**WEAKNESSES** ● Failure to achieve 3% energy resolution ● Insufficient PMT efficiency ● Insufficient detector/structure integrity ● Insufficient electronics/HV reliability ● Delay with detector installation
External	**OPPORTUNITIES** ● Supernova burst ● Diffuse Supernova background ● New physics	**THREATS** ● Underground collapse and flooding ● Lower than expected NPP thermal power

Table 8. JUNO SWOT table.

The JUNO experiment is expected to be a huge step forward in scale and precision among the reactor neutrino experiments. JUNO detector will be 20 times larger than the current largest reactor antineutrino detector KamLAND. Experiment requirements include maximal PMT coverage and 3% energy resolution at 1 MeV of released energy. Therefore the detector construction has a number of technical challenges:

- Creating an acrylic sphere to hold 20 kt of liquid scintillator which is inflammable.
- Production of high efficiency PMT tubes.
- Protection of PMTs against the shock wave.
- Potting and connecting PMTs and electronics underwater at depths up to 35 meters.
- At least 20 years working time (30 years expected).

All these items indicate high reliability and safety requirements. The potential risks are minimized by extensive subsystem testing and putting high reliability requirements on the detector components.

Construction of a large underground laboratory in Jiangmen has its own risks. Two major ones are the possibility of underground collapse or flooding. Both risks are

minimized by careful planning and adjustments of the civil construction work and timescale.

Preparing our proposal in 2017 there was a chance of delay or cancellation of two Taishan NPP cores construction which we mentioned in 2018-2020 SWOT analysis. In 2020 we recognized that indeed the construction date of these two cores is still undetermined and JUNO should be taking consequently a 25% longer (eight years instead of six) in order to achieve the required sensitivity to the neutrino mass hierarchy. This change is reflected elsewhere in this proposal.

JUNO has a very rich experimental program. In case of achievement of required energy resolution JUNO will measure mass hierarchy with statistical significance of 3-4 standard deviation. This measurement does not depend on any unknown oscillation parameters (such as CP-violating phase δ_{CP} or neutrino mixing angle θ_{23}). JUNO will measure oscillation parameters Δm^2_{21}, Δm^2_{32} and θ_{12} with sub-percent accuracy. The only input required is θ_{13} which will be measured by Daya Bay experiment with significant precision.

After KamLAND and BOREXINO, JUNO will be the third experiment to observe geoneutrinos. In ten years of data taking we expect 4000 geoneutrino which should be compared to today's world total 130. Other physical topics include studies of solar and atmospheric neutrinos, search for sterile neutrinos and new physics, etc.

In case of SN explosion JUNO will detect several thousands of events[33] in various channels — which will be a breakthrough in this field. In addition, JUNO has a potential of detecting diffuse Supernova neutrinos.

[33] for SN1987A-like Supernova in the center of our galaxy

6 Theses, publications, talks

6.1 Theses

Year	Type	Author	Title
2017	candidate	M. Gonchar	The measurement of neutrino mixing angle θ_{13} and neutrino mass splitting Δm^2_{32} in the Daya Bay experiment.
2017	doctor	D. Naumov	Measurement θ_{13} and Δm^2_{32} of and quantum-field theory of neutrino oscillations.
Soon	candidate	N. Anfimov	Methods for the research of photodetectors and their application.
Soon	doctor	I. Nemchenok	Development and research of plastic and liquid scintillators for detectors of experiments in the field of neutrino physics.
Soon	doctor	O. Smirnov	Study of the geo- and pp-chain solar neutrino fluxes with the Borexino detector.

Table 9. Past and future candidate and doctor theses.

6.2 Selected publications for 5 years

1. D.V.Naumov, V.A.Naumov, Quantum Field Theory of Neutrino Oscillations, 10.1134/S1063779620010050. Phys.Part.Nucl. 51 (2020) no.1, 1-106.
2. O.Smirnov, “Experimental aspects of geoneutrino detection: Status and perspectives”, Progress in Particle and Nuclear Physics 109 (2019) 103712.
3. A.Fatkina et al., GNA: new framework for statistical data analysis. [arXiv:1903.05567 [cs.MS]]. 10.1051/epjconf/201921405024. EPJ Web Conf. 214 (2019) 05024.
4. V.A.Bednyakov, D.V.Naumov, Coherency and incoherency in neutrino-nucleus elastic and inelastic scattering By Vadim A. Bednyakov, Dmitry V. Naumov. arXiv:1806.08768 [hep-ph]. 10.1103/PhysRevD.98.053004. Phys.Rev. D98 (2018) no.5, 053004.
5. A.Fatkina et al., CUDA Support in GNA Data Analysis Framework. [arXiv:1804.07682 [cs.DC]]. 10.1007/978-3-319-95171-3_2. Computational Science and Its Applications Proc. Part IV, p. 12-24 (2018).
6. N.Anfimov on behalf of the JUNO collaboration. Large photocathode 20-inch PMT testing methods for the JUNO experiment, JINST 12 (2017).
7. N.Anfimov, A.Rybnikov, and A.Sotnikov. Optimization of the light intensity for photodetector calibration. Nucl. Instrum. Meth., A939:61 – 65, 2019.
8. Daya Bay Collaboration, Extraction of the ^{235}U and ^{239}Pu Antineutrino Spectra at Daya Bay, arXiv:1904.07812 [hep-ex]. 10.1103/PhysRevLett.123.111801. Phys.Rev.Lett. 123 (2019) no.11, 111801.
9. Daya Bay Collaboration, A high precision calibration of the nonlinear energy

response at Daya Bay, arXiv:1902.08241 [physics.ins-det]. 10.1016/j.nima.2019.06.031. Nucl.Instrum.Meth. A940 (2019) 230-242.
10. Daya Bay Collaboration, Measurement of the Electron Antineutrino Oscillation with 1958 Days of Operation at Daya Bay, arXiv:1809.02261 [hep-ex]. 10.1103/PhysRevLett.121.241805. Phys.Rev.Lett. 121 (2018) no.24, 241805.
11. Daya Bay Collaboration, Improved Measurement of the Reactor Antineutrino Flux at Daya Bay, arXiv:1808.10836 [hep-ex]. 10.1103/PhysRevD.100.052004. Phys.Rev. D100 (2019) no.5, 052004.
12. Daya Bay Collaboration, Evolution of the Reactor Antineutrino Flux and Spectrum at Daya Bay, arXiv:1704.01082 [hep-ex]. 10.1103/PhysRevLett.118.251801. Phys.Rev.Lett. 118 (2017) no.25, 251801.
13. Daya Bay Collaboration, Measurement of electron antineutrino oscillation based on 1230 days of operation of the Daya Bay experiment, arXiv:1610.04802 [hep-ex]. 10.1103/PhysRevD.95.072006. Phys.Rev. D95 (2017) no.7, 072006.
14. Daya Bay Collaboration, Study of the wave packet treatment of neutrino oscillation at Daya Bay, arXiv:1608.01661 [hep-ex]. 10.1140/epjc/s10052-017-4970-y. Eur.Phys.J. C77 (2017) no.9, 606.
15. Daya Bay and MINOS Collaborations, Limits on Active to Sterile Neutrino Oscillations from Disappearance Searches in the MINOS, Daya Bay, and Bugey-3 Experiments. arXiv:1607.01177 [hep-ex]. 10.1103/PhysRevLett.117.209901, 10.1103/PhysRevLett.117.151801. Phys.Rev.Lett. 117 (2016) no.15, 151801, Addendum: Phys.Rev.Lett. 117 (2016) no.20, 209901.
16. Daya Bay Collaboration, Improved Search for a Light Sterile Neutrino with the Full Configuration of the Daya Bay Experiment, arXiv:1607.01174 [hep-ex]. 10.1103/PhysRevLett.117.151802. Phys.Rev.Lett. 117 (2016) no.15, 151802.
17. Daya Bay Collaboration, Measurement of the Reactor Antineutrino Flux and Spectrum at Daya Bay, arXiv:1508.04233 [hep-ex]. 10.1103/PhysRevLett.118.099902, 10.1103/PhysRevLett.116.061801. Phys.Rev.Lett. 116 (2016) no.6, 061801, Erratum: Phys.Rev.Lett. 118 (2017) no.9, 099902.
18. Daya Bay Collaboration, The Detector System of The Daya Bay Reactor Neutrino Experiment, arXiv:1508.03943 [physics.ins-det]. 10.1016/j.nima.2015.11.144. Nucl.Instrum.Meth. A811 (2016) 133-161.
19. JUNO Collaboration, Neutrino Physics with JUNO. arXiv:1507.05613 [physics.ins-det]. 10.1088/0954-3899/43/3/030401. J.Phys. G43 (2016) no.3, 030401.

6.3 Selected talks for 5 years

1. D.Naumov, plenary talk, New Results from the Daya Bay Reactor Neutrino Experiment.NeutrinoTelescopes,13-17 March 2017, Venice, Italy (plenary).
2. D.Naumov, plenary talk, Latest Results from the Daya Bay Reactor Neutrino Experiment . New Trends in High-Energy Physics, 2-8 October 2016, Budva, Becici, Montenegro (plenary).
3. D.Naumov, plenary talk, Neutrino Physics with Nuclear Reactors. QUARKS-2016 19th International Seminar on High Energy Physics, Pushkin, Russia, 29 May - 4 June, 2016 (plenary).
4. D.Naumov, plenary talk, Neutrino Physics with Nuclear Reactors. Международная Сессия-конференция Секции ядерной физики ОФН РАН, 12 - 15 апреля, 2016, ОИЯИ, Дубна (plenary).
5. D.Naumov, plenary talk, Neutrino Physics program at the JINR. 4th SOUTH AFRICA - JINR SYMPOSIUM. Few to Many Body Systems: Models and Methods and Applications, September 21-25, 2015, JINR Dubna, Moscow region, Russia (plenary).

6. A.Olshevskiy, Neutrino Physics Lectures, VII Conference for young scientist and specialists, Alushta, 11-18 June 2018
7. A.Olshevskiy, Invited Lecture on Neutrino Physics, The JINR 26th Summer School, 15 July 2019.
8. O.Smirnov, plenary talk, “Geoneutrino studies with JUNO detector”, International Workshop: Neutrino Research and Thermal Evolution of the Earth October 25 – 27, 2016, Sendai, Japan.
9. O.Smirnov, plenary talk, “Geo-neutrino : experimental status and perspectives”, Conference on Neutrino and Nuclear Physics (CNNP2017) 15-21 October 2017 Monastero dei Benedettini, University of Catania, Catania, Italy.
10. O.Smirnov, plenary talk, “Solar and geo-neutrinos: current status and future directions”, International School of Nuclear Physics, 41st Course Star Mergers, Gravitational Waves, Dark Matter and Neutrinos in Nuclear, Particle and Astro-Physics, and in Cosmology Erice-Sicily: September 16-24, 2019
11. O.Smirnov, plenary talk, “Solar and geo-neutrinos”, Future of large-scale neutrino detectors INR, Moscow: October 3-4, 2019
12. M.Gonchar, lecture, "JINR Neutrino Program", 10th Student School on Nuclear Physics, 14-16 May 2019, Borovets, Bulgaria.
13. O.Smirnov, lecture, “The JUNO experiment”, lecture at ISAPP doctorate school, Arenzano, Italy, June 21, 2017.
14. K.Treskov, parallel talk «The latest results from the Daya Bay», ICPPA-2018, October 22-26 2018, Moscow, Russia.
15. K.Treskov, parallel talk, «The impact of the carbon-14 contamination in liquid scintillator on the sensitivity to the neutrino mass hierarchy determination in the JUNO experiment with Global Neutrino Analysis framework» October 2-6 2017, Dubna.
16. K.Treskov, parallel talk, “Fast neutron background in the Daya Bay experiment”, AYSS-2016, Dubna, Russia
17. M.Gonchar, parallel talk, "Oscillation analysis in Daya Bay experiment". XIX International Scientific Conference of Young Scientists and Specialists. Dubna, 16-20 February, 2015.
18. M.Gonchar, parallel talk, “Recent results from Daya Bay experiment”. International session-conference of the section of nuclear physics of PSD RAS. Dubna, 12-15 April, 2016.
19. M.Gonchar, parallel talk, "Oscillation analysis in Daya Bay experiment", International School of Subnuclear Physics 56th Course: From Gravitational Waves to QED, QFD and QCD, Erice, Italy, 14-23 June, 2018.
20. M.Gonchar, parallel talk, "New results from the Daya Bay experiment", New Trends in High-Energy Physics, Becici, Budva, Montenegro, 24-30 September 2018.
21. M.Gonchar, parallel, "GNA — high performance fitting for neutrino experiments", Computing in High Energy Physics, 4-8 November 2019, Adelaide, Australia.
22. M.Gonchar, parallel, "The results of the Daya Bay experiment and the status of the JUNO experiment", International Session-Conference, Section of Nuclear Physics PSD RAS, 10-12 March 2020, Novosibirsk, Russia.
23. D.Naumov, parallel talk, Coherency and incoherency in elastic and inelastic neutrino-nucleus scattering. The Magnificent CEvNS Workshop 2018.
24. D.Naumov, parallel talk, Neutrino Oscillations in QFT with relativistic wave packets. Международная Сессия- конференция Секции ядерной физики ОФН РАН, 12 - 15 апреля, 2016, ОИЯИ, Дубна (parallel).
25. O.Smirnov, parallel talk, “Measurement of the geo-neutrino fluxes: status and future”, International Session-Conference of the Section of Nuclear Physics of the Physical Sciences Department of the Russian Academy of Sciences "Physics of

fundamental interactions" dedicated to 50th anniversary of Baksan Neutrino Observatory, June 6-8, 2017 (parallel).
26. N.Anfimov, parallel talk, . Large photocathode 20-inch PMT testing methods for the JUNO experiment. INSTR17: Instrumentation for Colliding Beam Physics. Novosibirsk, Russia.
27. K.Treskov, poster «GNA – high performance fitting framework for neutrino experiments», PhyStat-Nu 2019, January 21-25 2019, CERN, Geneve, Switzerland.
28. K.Treskov, poster «Experimental study of decoherence effects in neutrino oscillations in Daya Bay», Neutrino 2018, June 4-8 2018, Heidelberg, Germany.
29. K.Treskov, poster, 2016 European School of High-Energy Physics, “Inverse beta-decay event selection and fast neutron background in the Daya Bay experiment”.
30. M.Gonchar, poster, “Oscillation analysis in Daya Bay experiment”. Neutrino 2016. London 4-9 July, 2016.

7 Financial requests

The request of the project for the years 2021-2023 amounts to 3.2M USD.

This includes:

- 1.0M USD for detector operation
- 0.8M USD for travel expenses
- 0.5M USD for the JINR computing infrastructure upgrade
- 0.5M USD for the TAO detector photosensors purchase and tests
- 0.2M USD for the TopTracker mechanical support and installation
- 0.2M USD for HV Units contract amendments, installation and tests

The distribution of resources for different years is presented in Forms 26 and 29.

Форма № 26

Предлагаемый план-график и необходимые ресурсы для осуществления проекта JUNO

Наименование узлов и систем установки, ресурсов, источников финансирования			Стоимость узлов установки Потребности в ресурсах (тыс.$)	Предложения Лабораторий распределению финансиро и ресурсов		
				1 год	2 год	3 год
Основные узлы и оборудование	1. Эксплуатация детектора JUNO		1000	-	500	500
	2. Фотоприемники для ТАО детектора, приобретение и проверка		500	300	200	-
	3. Механическая структура Top Tracker: изготовление, сборка, установка		200	200	-	-
	4. ВВ система: дополнения к контракту, сборка, установка, проверка		200	200	-	-
	5. Вычислительная инфраструктура (серверы, диски для хранения данных)		500	300	100	100
Необходимые ресурсы	*Нормо-часы*	ОП ОИЯИ ООЭП ЛЯП	*2100* *2400*	*700* *800*	*700* *800*	*700* *800*
	тыс. долл.	Запуск, смены, анализ, участие в совещаниях и конференциях	800	300	250	250
Источники финансиро-вания	Бюджет	Бюджет	**3200**	**1300**	**1050**	**850**
	Внебюджет	Дополнительные вклады коллаборантов, гранты.	**30**	**10**	**10**	**10**

Руководитель проекта

Форма № 29

8 Смета затрат по проекту JUNO

№№ пп	Наименование статей затрат	Полная Стоимость Нормочасы Тыс. долл.	1 год	2 год	3 год
1.	Ускоритель	-	-	-	-
2.	ЭВМ	-	-	-	-
3.	Комп. связь (тыс. долл.)	30	10	10	10
4.	*ООЭП ЛЯП (нормочасы)* *ОП ОИЯИ (нормочасы)*	*2400*	*800*	*800*	*800*
5.	Материалы (тыс. долл.) Оборудование (тыс. долл.)	*2100*	*700*	*700*	*700*
6.	Оплата НИР (тыс. долл.) Командировочные расходы (тыс. долл.)	900	500	300	100
7.		1440	480	480	480
8.		30	10	10	10
9.		800	300	250	250
	Итого по прямым расходам (тыс. долл.)	**3200**	**1300**	**1050**	**850**

Руководитель Проекта

Директор Лаборатории

Ведущий инженер-экономист Лаборатории